Inhibition of KCa3.1 by Depolarisation and 2-Aminoethoxydiphenyl Borate (2-APB) During Ca^{2+} Release Activated Ca^{2+} (CRAC) Entry in Human Erythroleukemia (HEL) Cells: Implications for the Interpretation of 2-APB Inhibition of CRAC Entry

Robert Littlechild, Nathalie Zaidman*, Darren Khodaverdi& and Michael James Mason#

Department of Physiology, Development and Neuroscience, University of Cambridge, Downing Street, CB2 3EG, Cambridge UK.

Correspondence to: Dr. Michael J. Mason
Email: mjm39@cam.ac.uk
Telephone: 44 1223 333849
Fax: 44 1223 333840

* present address
CHU Charleroi
Neurosurgery
Boulevard Paul Janson, 92
6000 Charleroi
Belgium

& present address
Department of Emergency Medicine
Dunedin Hospital
201 Great King Street
Dunedin 9016
New Zealand

Keywords

2-APB, membrane potential, KCa3.1, HEL cells, CRAC channel, patch clamp, current clamp, intracellular Ca^{2+}

Abstract

In the present experiments in HEL cells, we have investigated the requirement for a hyperpolarised resting membrane potential for the initial activation of the Ca^{2+} activated K^+ channel, KCa3.1, following activation of the Ca^{2+} release activated Ca^{2+} (CRAC) entry pathway. In intact cells, fluorimetric measurements of $[Ca^{2+}]_i$ following thapsigargin-mediated activation of CRAC entry revealed a sustained increase in $[Ca^{2+}]_i$. Block of KCa3.1 by application of charybdotoxin resulted in a 50% reduction in the steady-state $[Ca^{2+}]_i$, consistent with the well established role for KCa3.1-mediated hyperpolarisation in augmenting CRAC entry. Interestingly, subsequent depolarisation to 0 mV by application of gramicidin resulted in a fall in steady-state Ca^{2+} levels to values theoretically below that required for activation of KCa3.1. Whole cell patch clamp experiments confirmed the lack of KCa3.1 activation at 0 mV following activation of the CRAC entry pathway, indicating an absolute requirement for a hyperpolarised resting membrane potential for the initial activation of KCa3.1 leading to hyperpolarsation and augmented Ca^{2+} entry. Current clamp experiments confirmed the requirement for a hyperpolarised resting membrane potential in KCa3.1 activation by CRAC entry. Given the critical role played by KCa3.1 and membrane potential in general in the control of CRAC-mediated $[Ca^{2+}]_i$ changes, we investigated the hypothesis that inhibition of the CRAC-mediated changes in $[Ca^{2+}]_i$ observed following 2-APB addition may in part arise from direct inhibition of KCa3.1 by 2-APB. Under whole cell patch clamp, 2-APB, at concentrations typically used to block the CRAC channel, potently inhibited KCa3.1 in a reversible manner (half maximal inhibition 14.2 μM). This block was accompanied by a marked shift in the reversal potential to depolarised values approaching that set by endogenous membrane conductances. At the single channel level, 2-APB applied to the cytosolic face resulted in a significant reduction in open channel

probability and a fall in the mean open time of the residual channel activity. Our data highlight the absolute requirement for a hyperpolarising resting membrane conductance for the initial activation of KCa3.1 by CRAC entry. Additionally, our results document direct inhibition of KCa3.1 by 2-APB, thus highlighting the need for caution when ascribing the site of inhibition of 2-APB exclusively to the CRAC entry pathway in experiments where membrane potential is not controlled.

1. Introduction

Ca^{2+} entry mediated by depletion of endosomal Ca^{2+} stores in non-excitable cells is a ubiquitous mechanism leading to Ca^{2+} mediated down-stream signaling events. The role of intracellular stores in regulation of the Ca^{2+} permeability of the plasma membrane was first highlighted by Putney and co-workers in 1986 [1]. Store operated Ca^{2+} entry (SOCE) as it has subsequently come to be known has since been under extensive investigation and has moved from the observation of augmented Ca^{2+} entry following depletion of endosomal Ca^{2+} stores [1], to detection of an inward Ca^{2+} current accompanying store depletion [2], to the more recent identification of several components of the transduction and pore-forming elements including Orai1, 2 and 3 and Stim1 and 2 which signal the Ca^{2+} loss from endosomal compartments to the Orai components in the plasma membrane [as reviewed in 3]. The best electrophysiologically studied variant of the current is the calcium release activated Ca^{2+} (CRAC) channel, first isolated by Hoth and Penner [2] in rat basophilic leukemia cells and later by Zwiefach and Lewis [4] in Jurkat cells. This current displays marked inward rectification thus making net Ca^{2+} entry particularly susceptible to depolarisation.

SOCE pathways and CRAC entry in particular, play important roles in health and disease [as reviewed in 5]. As such, Ca^{2+} entry pathways controlled by the Ca^{2+} status of intracellular Ca^{2+} stores are important targets for therapeutic modulation. To date, high affinity, selective blockers of the signaling cascade leading to SOCE have remained elusive. Numerous organic compounds are known to block CRAC currents and inhibit elevations in $[Ca^{2+}]_i$ ascribed to Ca^{2+} entry by these pathways [as reviewed in 5]. 2-aminoethoxyphenyl borate (2-APB) is a well established blocker of CRAC currents [6,7,8]. Its ability to modulate CRAC currents is complex. At low concentrations it has been shown to augment

channel conductance while at high concentrations it is inhibitory [7]. As this compound became more widely used as a SOC/CRAC entry blocker its off target effects began to mount up. These include block of endosomal Ca^{2+} pumps [9], voltage-gated K^+ channels [10], the non-selective cation channel TRPM7 [11], a Mg^{2+}-inhibited K^+ conductance described in human erythroleukemia (HEL) cells [12] and mitochondrial Ca^{2+} release [7]. Although it is well established to block CRAC currents at higher concentrations, its additional inhibitory influences make for cautious interpretation of effects observed during 2-APB application. This is particularly important when ascribing a site of action of this agent.

In the present experiments we have undertaken experiments to investigate the requirement for a hyperpolarised resting potential in ensuring adequate CRAC-mediated changes in $[Ca^{2+}]_i$ for activation of KCa3.1 in HEL cells. Our results highlight the absolute requirement for a hyperpolarised potential while confirming a critical role for the hyperpolarisation mediated by the Ca^{2+}-activated K^+ channel, KCa3.1 in maximising Ca^{2+} entry. Importantly, we demonstrate that 2-APB potently inhibits KCa3.1, independent of its effects on CRAC channel function and propose that inhibition of KCa3.1 may underlie, in part, the inhibitory influence of 2-APB on Ca^{2+} elevations mediated by CRAC entry in experiments in which membrane potential is not controlled.

2. Materials and Methods

2.1. Reagents

NaCl and KCl were purchase from Fisher Scientific (Loughborough, Leicestershire, UK) or Sigma-Aldrich Ltd (Gillingham, Dorset, UK). $MgCl_2$, HEPES, N-methyl-D-glucamine ($NMDG^+$), EGTA, NaOH, KOH, DMSO, ethyl alcohol, gramicidin D and 2-aminoethoxydiphenyl borate (2-APB), were purchased from Sigma-Aldrich Ltd. $CaCl_2$ was purchased from VWR International (Lutterworth, Leicestershire, UK). D-glucose was

purchased from Fissons Scientific Apparatus (Loughborough, Leicestershire, UK). Thapsigargin and ionomycin were purchased from Merck Biosciences Calbiochem (Nottingham, Nottinghamshire, UK). Charybdotoxin was purchased from Bachem (St. Helens, Merseyside, UK). The acetoxymethyl ester of Fluo3 (Fluo3-AM) was purchased from TeFlabs (Austin, Tx, USA). Pluronic was obtained from Molecular Probes (Leiden, NL). 2-APB and thapsigargin were made up as concentrated stocks in DMSO while ionomycin and gramicidin D were made up in ethyl alcohol. Fluo3-AM was made up in a pluronic/DMSO solution.

2.2. Cell culture

HEL cells, a human erythroleukemia cell line [13] were originally obtained from the European Collection of Animal Cell Cultures (Porton Down, Salisbury, UK). Cells were propagated in HCO_3^--buffered RPMI 1640 media supplemented with 10% fetal bovine serum, 4 mM L-glutamine, 100 U.ml^{-1} penicillin and 50 μg.ml^{-1} streptomycin (all from Sigma-Aldrich Ltd., Dorset, UK or Invitrogen, Paisley, UK) in a humidified atmosphere of 95% air, 5% CO_2 at 37°C. Cells grew in suspension and were passaged twice a week.

2.3. Solutions

2.3.1. Fluo3 measurements of $[Ca^{2+}]_i$

The basic extracellular Na^+ solution had the following composition in mM; 145 NaCl, 5 KCl, 1 $CaCl_2$, 1 $MgCl_2$, 10 Glucose, 0.1 EGTA, 10 HEPES. The solution was titrated to pH 7.35 with NaOH. Na^+-free solution was made by equimolar replacement of Na^+ with $NMDG^+$. This solution was titrated to pH 7.35 with $NMDG^+$ free base.

2.3.2. Whole cell patch clamp

For whole cell recording, the standard low Ca^{2+}, KCl-based pipette solution contained (mM) 150 KCl, 0.15 EGTA, 1 $MgCl_2$, 10 HEPES adjusted to pH 7.2 with KOH. This solution did not support activation of KCa3.1 in the absence of elevated cytosolic free Ca^{2+}. In a small subset of experiments EGTA was omitted from this solution as noted in the text. In some experiments free Ca^{2+} was buffered to 5 μM. This solution had the following composition in mM; 150 KCl, 5 EGTA, 4.8329 $CaCl_2$, 1.0074 $MgCl_2$, 10 HEPES adjusted to pH 7.2 with KOH. The values for Ca^{2+} and Mg^{2+} are theoretical concentrations that must be added to yield 5 μM free Ca^{2+} and 1 mM free Mg^{2+}, as determined by WEBMAXC with extended constants (http://maxchelator.stanford.edu/webmaxc/webmaxcE.htm). The basic extracellular Na^+ solution had the following composition in mM; 145 NaCl, 5 KCl, 1 $CaCl_2$, 1 $MgCl_2$, 10 Glucose, 10 HEPES. The solution was titrated to pH 7.35 with NaOH. When required Ca^{2+} was omitted from the solution.

For current clamp experiments, the low Ca^{2+}, KCl-based pipette solution contained (mM) 150 KCl, 0.1 EGTA, 2 $MgCl_2$, 10 HEPES adjusted to pH 7.2 with KOH. In some experiments EGTA was omitted from this solution. The extracellular Na^+ solutions were identical to that used in the whole cell voltage clamp experiments with the exception that the Ca^{2+}-free solution was supplemented with 0.1 mM EGTA.

2.3.3. Excised inside-out single channel patch clamp recordings

The NaCl-based pipette solution is identical to the standard NaCl-based extracellular solution used for whole cell recordings. The standard KCl-based solution used to bath the cytosolic face of the excised patch had the following composition in mM; 150 KCl, 5 EGTA, 4.8044 $CaCl_2$, 5 EGTA, 5.0368 $MgCl_2$, 10 HEPES and was adjusted to pH 7.2 by titration

with KOH. These theoretical $CaCl_2$ and $MgCl_2$ concentrations were added to yield 5 μM free Ca^{2+} and 5 mM free Mg^{2+} as determined by WEBMAXC with extended constants. When required the concentrations of total Ca^{2+} and Mg^{2+} were altered to yield solutions of defined free Ca^{2+} and Mg^{2+} in accordance with the values obtained from WEBMAXC with extended constants.

2.3.4. Solution changes and additions

In whole cell and excised patch clamp experiments solution changes were made by gravity fed superfusion of the chamber. Under voltage clamp, thapsigargin was applied by superfusion of thapsigargin containing solution from a large bore pipette positioned close to the cell. In current clamp experiments thapsigargin was applied by gravity fed superfusion of the chamber.

In cuvette based experiments reagents were added directly to the cuvette from concentrated stocks.

2.4. Patch clamp methods

2.4.1. Recording

Cells were added to a low volume plexiglass chamber mounted on the stage of an inverted microscope. The bottom of the chamber was formed by adherence of a glass cover slip with silicone grease. The chamber was grounded via a Ag/AgCl wire placed directly in the chamber downstream of the cells. Tight seal whole cell patch clamp recordings in voltage and current clamp modes and excised single channel recordings were carried out using an Axopatch 200A amplifier (Molecular Devices, Union City, CA, USA). 70% series resistance compensation was achieved in whole cell recordings using the series resistance compensation feature of the amplifier. Electrodes were pulled from filamented borosilicate

glass (Harvard Apparatus, Kent, UK) and the tips fire polished. Electrodes had resistances of 3 to 8 MΩ when filled with standard KCl-based internal for whole cell recordings and 10 to 14 MΩ when filled with NaCl-based solution for excised patch recordings. All experiments were performed at room temperature (20-24^{o}C).

2.4.2. *Data acquisition*

Amplifier control and data acquisition were performed using Axograph 4.9 software (Axograph Scientific, Sydney, Australia) running on a Macintosh computer using a Digidata 1322A 16 bit data acquisition system (Molecular Devices, Union City, CA, USA). Analysis was performed using Axograph and custom macros and procedures written within IGOR Pro (Wavemetrics, Lake Oswego, OR, USA).

In whole cell voltage clamp recordings, 200 ms voltage ramps from -100 to +100 mV were applied every 3 s from a holding potential of -80 or 0 mV. Between ramps the cell was held at the indicated holding potential. The voltage clamp and current clamp data were filtered at 1 kHz using the 4 pole Bessel filter of the Axopatch 200A amplifier and acquired at 2 kHz. Reversal potentials were extracted from each voltage ramp using a custom macro written in IGOR Pro. All data presented are the raw whole cell currents uncorrected for the presence of background currents.

Excised single channel data were filtered at 1 kHz and acquired at 10 kHz.

2.4.3. Analysis

When required, single channel activity was quantified using all-points-amplitude histograms produced using the built in histogram routine within IGOR Pro with a current bin width of 0.05 pA. The calculated amplitude histograms were fit to the sum of multiple Gaussian distributions using the multi-peak fitting routine within IGOR Pro as previously

reported [14.15]. The calculated areas, A, of the individual Gaussian peaks in the multipeak fit were taken directly from the output of the peak fitting routine and used to calculate NPo were N is the number of channels and Po is the open channel probability as previously reported by our laboratory [14,15]. Assuming all channels are identical and behave independently, NPo can be determined from the areas of individual Gaussian peaks using the following relationship [16] as modified from Selyanko *et. al.* [17] and Li *et. al.* [18]:

$$NPo = \frac{\sum_{i=0}^{N} iA_i}{\sum_{i=0}^{N} A_i}$$

where A_i is the area of the corresponding Gaussian peak for i open channels and N is the number of current levels in the patch as determined by the number of Gaussian peaks corresponding to multiples of the unitary single channel current.

For single channel open time analysis, the durations of channel openings were determined by detecting channel openings and closings using a 50% threshold crossing method [19] using a custom procedure written within IGOR Pro as previously reported [15]. The mean open time was directly calculated from the observed distributions of open times using the output of the IGOR Pro procedure. Mean open times were calculated from patches in which only a single channel was detected. Prior to analysis, the original data filtered at 1 kHz, was digitally filtered at 500 Hz using the Gaussian filter within Axograph. This was necessary to minimise spurious events associated with the signal to noise ratio of our acquired data. To ensure that brief openings associated with residual noise events did not bias the results, identical record lengths were analysed in the control and 2-APB conditions. All open events including the very briefest detectable events were included in the mean open time calculation. Given the filter frequencies used in this analysis brief events will be under-represented. As a result, the mean open times are over estimates, particularly in the presence

of 2-APB where the channel openings were subsequently shown to be significantly shorter.

In the whole cell experiments initiated with KCl-based pipette solutions and NaCl-based bath solutions, a +3 mV junction potential exists [20]. For the excised inside-out single channel data initiated with NaCl-based pipette solution and a KCl-based bath solution a -3 mV junction potential potential exists [20]. This results in all reported voltages being +3 mV more positive than actually applied. For presentation purposes, single channel data recordings have been smoothed using a binomial smoothing function within IGOR Pro. With the exception of the data used in the open channel time analysis, which was additionally filtered at 500 Hz post acquistion, all other data used in our analyses was filtered only at the level of the Axopatch 200A amplifier.

2.5. Measurements of intracellular $[Ca^{2+}]_i$ in cell suspensions

$[Ca^{2+}]_i$ was measured fluorimetrically in cell suspensions using fluo3 as previously reported [21]. 25 X 10^6 cells.ml^{-1} were incubated with 3 μM fluo3-AM (0.06% pluronic made up in DMSO) for 25 minutes at 37^{o}C. Cells were then centrifuged, resuspended in basic Na^+ solution and stored in the dark at room temperature until required. For intracellular Ca^{2+} measurements cells were centrifuged and added directly to a cuvette to give a final concentration of between 1 and 2 X 10^6 cells.ml^{-1} and fluo3 fluorescence monitored under continual stirring in a cuvette-based fluorescence spectrophotometer (Cairn Research Ltd, Faversham, Kent, UK) (Ex 488 nm, 10 nm half band width, Em 530 nm longpass, Comar Instruments, Cambridge, Cambridgeshire, UK). The photomultiplier tube output was externally filtered a 15 Hz using a lowpass Bessel filter (Frequency Devices Inc., Haverhill, MA, USA) and sampled at 30 Hz using the same data acquistion hardware and software and computer control as employed for the patch clamp measurements. To calibrate

the fluo3 signal the maximum fluorescence in the presence of saturating Ca^{2+} (F_{max}) and the minimum fluorescence in the complete absence of Ca^{2+} (F_{min}) is required. At the end of each experiment maximum fluorescence was determined by the addition of ionomycin in the presence of 16 mM Ca^{2+}. This was followed by the addition of 8 mM Mn^{2+} leading to quenching of the fluo3 signal (F_{Mn}). In cell free experiments the decline in fluorescence from F_{max} observed by addition of Mn^{2+} is consistently 89% of the decline observed by complete removal of Ca^{2+} (F_{min}) [21]. This relationship was used to calculate the minimum fluorescence value of fluo3 for each experiment. $[Ca^{2+}]_i$ for a given fluorescence (F) was then calculated according to the following relationship:

$$[Ca^{2+}]_i = 390 \times \frac{(F - F_{min})}{(F_{max} - F)}$$

Where F_{min} is the calculated minimum fluorescence in the absence of Ca^{2+}, F_{max} is the maximum fluorescence in the presence of ionomycin and 16 mM extracellular Ca^{2+}, and 390 is the dissociation constant for fluo3 in nM as defined by the manufacturer.

All experiments were performed at room temperature, 20-22^{o}C.

2.6. Analysis of the concentration dependence of 2-APB block of KCa3.1

For determination of the concentration dependence of 2-APB block of KCa3.1 the magnitude of the whole cell current at 0 mV, extracted from voltage ramps applied every second, was normalised to the magnitude of the current in the absence of 2-APB and fit to the following modified Hill equation;

$$Y = Baseline + \left(\frac{(1 - Baseline)}{(1 + ([2APB] / K_{1/2})^{n})} \right)$$

Where *Baseline* is the normalised 2-APB-insensitive whole cell current, (1-*Baseline*) is the maximal inhibition of the 2-APB-sensitive current, $K_{1/2}$ is the concentration of 2-APB that yields half maximal inhibition, and *n* is the apparent cooperativity of the process.

2.7 Statistical analysis and presentation

Data are presented as the mean ± the SEM. All error bars on graph symbols denote the SEM. Differences were considered statistically significant at the $p \leq 0.05$ level using paired Student's T-tests or repeated measures ANOVAs with Tukey-Kramer multiple comparison tests used to determine pairwise differences when required.

3. Results

3.1. Reversal by 2-APB of the thapsigargin-mediated rise in $[Ca^{2+}]_i$ in intact HEL cells

The influence of the established CRAC channel blocker 2-APB on Ca^{2+} signaling in HEL cells was investigated. Thapsigargin-induced activation of the CRAC channel in HEL cells was accompanied by a robust increase in $[Ca^{2+}]_i$. Figure 1A shows a representative experiment from a cell suspension where the CRAC entry pathway was activated by thapsigargin-mediated depletion of intracellular Ca^{2+} stores as previously reported by our laboratory [22]. Application of 75 μM 2-APB at the peak of the rise in Ca^{2+}_i resulted in a fall in free Ca^{2+} to near pre-thapsigargin levels. Such observations are consistent with the established interpretation in the literature that 2-APB inhibits Ca^{2+} entry via block of the CRAC entry pathway [7]. In 9 experiments thapsigargin induced a 260± 56 nM increase in Ca^{2+}_i over resting levels. 75 μM 2-APB significantly reduced the Ca^{2+} rise to 22 ± 6 nM

over baseline values ($p \leq 0.05$, n=9). This represents a 90 ± 3 % decrease in the thapsigargin-mediated rise in $[Ca^{2+}]_i$.

3.2. Effect of membrane potential on the thapsigargin-mediated changes in $[Ca^{2+}]_i$ in intact cells

In contrast to the direct pharmacological inhibition of the CRAC channel by 2-APB, changes in membrane potential can also have marked influences on CRAC channel-mediated Ca^{2+} changes as a result of the electrogenic nature of the entry pathway and the inwardly rectifying current-voltage relationship [2,4,22]. The role of membrane potential modulation of CRAC-mediated Ca^{2+} entry in HEL cells is of particular importance given the depolarised resting membrane potential and the expression of the Ca^{2+}-activated K^+ channel, KCa3.1 [12,14,15,23). We have investigated the role of the resting membrane potential and subsequent hyperpolarisation driven by activation of the Ca^{2+}-activated K^+ channel, KCa3.1, in the activation and modulation of the elevation in $[Ca^{2+}]_i$ mediated by thapsigargin. In Figure 1B, 200 nM charybdotoxin, a potent inhibitor of KCa3.1 in HEL cells [14,23] was added near the peak of the rise in $Ca^{2+}{}_i$. Addition of the toxin was accompanied by a marked fall in $[Ca^{2+}]_i$ to a value approximately 50% of the Ca^{2+} rise. In 9 experiments thapsigargin induced a 317 ± 27 nM increase in Ca^{2+} over resting levels. Charybdotoxin significantly reduced this increase to 153 ± 15 nM, a 51 ± 3% decrease in the thapsigargin-mediated rise in $[Ca^{2+}]_i$ ($p \leq 0.05$, n=9). Charybdotoxin's inhibitory influence on the Ca^{2+} response most likely arises from the inhibition of the hyperpolarising influence of KCa3.1 activated by the rise in $[Ca^{2+}]_i$ [14,23]. Assuming that 200 nM charybdotoxin maximally inhibits KCa3.1, the residual elevation in $[Ca^{2+}]_i$ is accounted for by the maintenance of a

residual membrane potential sufficient to support net Ca^{2+} entry.

To substantiate this interpretation, we have exploited the use of gramicidin, a monovalent cation selective pore forming antibiotic [as reviewed in 24]. In standard extracellular Na^+ solution gramicidin addition will clamp membrane potential at a value close to 0 mV, while in the absence of extracellular Na^+ (substituted with the impermeant monovalent cation NMDG), gramicidin will hyperpolarise the membrane potential to the theoretical value of -88 mV (K^+ equilibrium potential) [25,26]. Since the experiment presented in Panel B was perfomed in a Na^+ containing solution, subsequent addition of gramicidin abolishes the transmembrane potential attributable to the residual membrane conductance. This is accompanied by a fall in free Ca^{2+} towards pre-thapsigargin levels. Identical experiments were performed in the absence of extracellular Na^+ (equimolar substitution with NMDG). Again, charybdotoxin resulted in a marked fall in the thapsigargin-mediated rise in $[Ca^{2+}]_i$. However, in contrast to the effect of gramicidin shown in the presence of extracellular Na^+ (Figure 1B), subsequent addition of gramicidin resulted in a marked increase in $[Ca^{2+}]_i$ consistent with gramicidin-mediated hyperpolarisation to the theoretical value of -88 mV (Figure 1C). The mean data from 3 independent experimental series are shown in Figure 1D. Replacement of extracellular Na^+ with $NMDG^+$ had no significant effect on resting free $[Ca^{2+}]$, the peak increase in $[Ca^{2+}]_i$ induced by thapsigargin or the magnitude of the fall in $[Ca^{2+}]_i$ following charybdotoxin addition. However, application of gramicidin resulted in a significantly greater steady-state $[Ca^{2+}]$ when applied in NMDGCl extracellular solution ($p \leq 0.05$, n=3), a result we ascribe to the marked difference in membrane potential set by gramicidin in Na^+ and $NMDG^+$ solutions. In NMDGCl solution the steady-state $[Ca^{2+}]$ after gramicidin addition was not significantly different from that measured in the presence of KCa3.1 activity at the peak of

the thapsigargin response.

These data highlight the established importance of KCa3.1-mediated hyperpolarisation in maximising net Ca^{2+} entry during activation of the CRAC entry pathway. Importantly, these results highlight the need for a hyperpolarised resting membrane potential to ensure adequate Ca^{2+} entry sufficient for the activation of KCa3.1. Abolishing this transmembrane potential with gramicidin resulted in free Ca^{2+} falling to 106 ± 2.6 nM (n=3), a value that is not expected to activate KCa3.1 [23,27,28,29].

3.3. Membrane potential modulation of CRAC-mediated activation of KCa3.1 recorded under whole cell patch clamp

To more directly address the requirement for a hyperpolarised resting membrane potential for activation of KCa3.1 by CRAC Ca^{2+} entry, we have undertaken whole cell patch clamp experiments. We monitored the whole cell current attributed to KCa3.1 during application of thapsigargin with the magnitude of the current providing an index of the sub membranous Ca^{2+} level rather than the measure of global Ca^{2+} reported in Figure 1. By altering the holding potential between voltage ramps administered every 3 seconds and monitoring the magnitude of the KCa3.1 current it is possible to determine if a hyperpolarised membrane potential is required for the generation of sufficient CRAC entry for activation of KCa3.1. In Figure 2 a cell was whole cell patched using KCl-based, low Ca^{2+} solution containing 154 mM KCl. As noted in Materials and Methods, this solution has a resting free [Ca^{2+}] that does not support activation of KCa3.1. Importantly, solutions of near identical Ca^{2+} buffering capacity have been previously demonstrated by our laboratory to support robust Ca^{2+} signaling including receptor-mediated Ca^{2+} oscillations and oscillations in KCa3.1 activity [30,31,32]. Following transition to the whole cell configuration the cell was held at -80 mV and 200 ms voltage ramps from -100 to +100 mV

administered every three seconds. The magnitude of the ramp current at 0 mV was extracted from individual ramps and plotted in Panel A as a function of time. We have chosen to plot the current at 0 mV since the pipette solution used in these experiments supports variable levels of activation of TRPM7 as previously reported by our laboratory [12]. Since TRPM7 has a reversal potential near 0 mV, the magnitude of the outward current at this potential cannot be ascribed to TRPM7. A representative IV relationship before application of thapsigargin is shown in Figure 2B1. The traces labeled 1 through 4 in Panel B refer to the ramp currents at the indicated time points presented in Panel A. Application of thapsigargin was accompanied by a marked increase in the 0 mV current magnitude (Panel A) consistent with the pronounced increase in ramp current shown in Panel B2. This ramp current has the well defined characteristics of KCa3.1 in HEL cells as previously reported by our laboratory [14]. Changing the holding potential between ramps from -80 to 0 mV was accompanied by a large decline in the current to a new steady-state value near that recorded before thapsigargin application (as seen in Panels A and B3). Such a finding is consistent with the fall in global $[Ca^{2+}]_i$ observed in Figure 1 during gramicidin-induced clamp of membrane potential to 0 mV. Returning the holding potential to -80 mV was associated with an increase in current, again, consistent with augmented Ca^{2+} entry and the activation of KCa3.1. The extent of the return in current was variable, consistent with our finding of a marked cell to cell variability in the inactivation characteristics of KCa3.1 and possibly of the CRAC entry pathway its self. To substantiate the role of modulation of Ca^{2+} entry in these holding potential changes in KCa3.1 activation, we subsequently removed extracellular Ca^{2+}. This resulted in a slow decline in KCa3.1 current as shown in Panel A at 0 mV and in Panel B4 across the entire voltage range of the ramp. The effect of 0 and -80 mV holding potentials on the magnitude of outward ramp current measured at 0 mV is summarised for 9 cells in Panel C. The current at 0 mV is normalised to the peak current recorded at a holding potential of -

80 mV during the initial application of thapsigargin. 0 mV holding potential resulted in a significant decline in the outward current at 0 mV to a value 13.7 ± 4.0% of the value recorded at -80 mV ($p \leq 0.05$, n=9). The magnitude of the current recorded at a holding potential of 0 mV during thapsigargin application was not significantly different than that recorded at -80 mV in the absence of thapsigargin ($p \geq 0.05$, n=9). Such a finding is consistent with no appreciable activation of KCa3.1 when the membrane potential was held at 0 mV, a result attributable to insufficient sub membranous Ca^{2+} levels for activation of KCa3.1. In spite of the large inward chemical Ca^{2+} gradient, membrane hyperpolarisation is an absolute requirement for sufficient Ca^{2+} entry for the activation of KCa3.1.

Whole cell current clamp experiments were undertaken that further substantiate the critical role played by the resting membrane potential in the initial activation of KCa3.1. In the experiment presented in Figure 3A a cell in whole cell current clamp mode was superfused with Ca^{2+}-free Na^{+} solution containing 200 nM thapsigargin. Prior to thapsigargin, the resting membrane potential was approximately -23 mV. Depletion of intracellular Ca^{2+} stores was accompanied by a marked transient hyperpolarisation to approximately -84 mV followed by a return to a resting potential of approximately -19 mV. The transient nature of the hyperpolarisation is attributable to transient activation of the Ca^{2+}-activated K^{+} conductance, secondary to the transient rise in free Ca^{2+} arising from extrusion of Ca^{2+} from the cytosol (see supplemental Figure S1). In accordance with this interpretation, thapsigargin addition in the presence of extracellular Ca^{2+} is accompanied by a sustained hyperpolarisation consistent with sustained CRAC-mediated Ca^{2+} entry (see supplemental Figure S2). In the experiment presented in Figure 3, re-introduction of 1 mM extracellular Ca^{2+} was accompanied by a marked hyperpolarisation of the cell to a value of -84 mV, consistent with CRAC-mediated Ca^{2+} entry leading to activation of KCa3.1. In a

subset of cells, (6 of 18), reintroduction of Ca^{2+} was not accompanied by hyperpolarisation. An example of such a response in shown in Figure 3B. In this experiment thapsigargin application transiently hyperpolarised the cell from approximately -27 mV to -79 mV, followed by recovery of the potential to a value of -8 mV immediately before Ca^{2+} re-introduction. One explanation for the lack of hyperpolarisation following Ca^{2+} reintroduction is that net Ca^{2+} entry in this cell is inadequate to activate KCa3.1. Consistent with this hypothesis, application of a small injection current sufficient to hyperpolarise, and hence increase the Ca^{2+} driving force, was accompanied by a secondary hyperpolarisation that persisted when the injection current was removed. This result is easily explained by the augmented Ca^{2+} entry accompanying the injection current-mediated hyperpolarisation leading to sufficient net Ca^{2+} entry for activation of KCa3.1. We have compared the resting membrane potential immediately prior to Ca^{2+} re-introduction in cells that hyperpolarised with those that required current injection to facilitate hyperpolarisation. Cells that hyperpolarised without injection current had a membrane potential of -18.0 ± 3.6 mV (n=12). In contrast, cells requiring an injection current had a significantly more depolarised potential of -5.8 ± 1.9 mV (n=6, $p \leq 0.05$). These data reinforce the requirement for adequate driving force to support sufficient Ca^{2+} entry for the initial activation of KCa3.1.

These whole cell patch clamp experiments were undertaken with a pipette solution containing 150 μM EGTA. While this solution has been documented to support robust Ca^{2+} signaling [30,31,32], it was necessary to ensure that the inhibitory influence of depolarisation of KCa3.1 activation was not an effect arising from augmented exogenous Ca^{2+} buffering power. Experiments were undertaken with a pipette solution of identical ionic composition but devoid of EGTA. Under these conditions indistinguishable results were observed. Figure

4 shows such an experiment. Panel A shows the whole cell ramp currents at a holding potential of -80 and 0 mV following thapsigargin application. Consistent with the data presented in Figure 2, a holding potential of 0 mV was accompanied by a marked decline in whole cell current and a shift in the reversal potential to a depolarised value. The influence of membrane potential on KCa3.1 regulation was also investigated under current clamp in the same cell (Panel B). The first segment of the recording in Panel B shows the transition from voltage clamp to current clamp following abolition of the KCa3.1 current by applying the voltage ramps from a holding potential of 0 mV. Transition to current clamp from a holding potential of 0 mV was accompanied by an immediate shift in potential to approximately -30 mV; a value set by the residual membrane conductances (see reversal potential in Panel A). This was followed by a secondary hyperpolarisation towards a value set by the activation of KCa3.1, driven by the Ca^{2+} entry supported by the hyperpolarised membrane potential. To confirm this interpretation, the cell was again placed in voltage clamp and ramps applied from a holding potential of 0 mV to inactivate KCa3.1 (data not shown). Upon return to current clamp the cell displayed a similar membrane potential of approximately -30 mV as shown in the second segment of the record in Panel B. In this experiment, however, the cell was immediately depolarised to approximately 0 mV by the application of a small injection current of approximately 11 pA. At 0 mV membrane potential no secondary hyperpolarisation was observed. Removal of the injection current resulted in a small hyperpolarisation to approximately -25 mV and the development of the secondary hyperpolarisation consistent with sufficient Ca^{2+} entry and the activation of KCa3.1. Taken in concert, these data demonstrate that the influence of depolarisation on KCa3.1 inhibition does not arise as a result of the presence of 150 μM EGTA in the internal pipette solution while highlighting the need for a hyperpolarised potential for sufficient Ca^{2+} influx to activate KCa3.1.

3.4. Direct inhibition by 2-APB of KCa3.1 recorded under whole cell patch clamp

Given the requirement for KCa3.1 activation for optimisation of CRAC entry, could the fall in $[Ca^{2+}]_i$ observed during 2-APB addition have a component of block of KCa3.1? To address this question it is imperative that activation of KCa3.1 be independent of any CRAC entry which is well established to be inhibited by 2-APB [6,7,8]. In an effort to meet this criteria, we added 5 μM free $[Ca^{2+}]$ to the whole cell patch pipette (see Materials and Methods). Following transition to the whole cell configuration, a robust KCa3.1 current was detected. Figure 5A shows the time course of changes in the whole cell ramp current at 0 mV extracted from voltage ramps administered every 3 s following activation of KCa3.1. Changing the holding potential from -80 to 0 mV did not result in the significant decline in whole cell current observed during thapsigargin application as shown in Figure 2. In fact, the current recorded at a holding potential of 0 mV was augmented in some cells over that recorded at -80 mV. Such an observation is consistent with the modulation of the KCa3.1 channel by depolarisation previously reported in HEL cells by our laboratory [14,15]. Removal of extracellular Ca^{2+} had no significant effect upon the magnitude of the KCa3.1 current consistent with the conclusion that CRAC entry has no detectable role in Ca^{2+}-mediated activation of KCa3.1 when cells are dialysed with 5 μM free $[Ca^{2+}]$ under the present conditions. Under these conditions addition of 75 μM 2-APB was accompanied by near complete abolition of the outward current recorded at 0 mV and attributed to KCa3.1 as shown in Figure 6A. Representative IV relationships before and during application of 2-APB at the indicated time points marked in Panel A, are shown in Panel B. In Panel C we have summarised the influence of 75 μM 2-APB on the whole cell ramp current recorded at 0 mV in 8 cells. The current at 0 mV has been normalised to the magnitude of the current at -80 mV holding potential immediately prior to addition of 2-APB. While changing the holding

potential from -80 to 0 mV resulted in a small increase in KCa3.1 in some cells as previously reported [14,15], this effect was not statistically significant in this data set. Subsequent addition of 75 μM 2-APB resulted in a significant decline in the current at 0 mV to a value 11.6 ± 4.5 % of the control value in the absence of 2-APB ($p \leq 0.05$, n=8). Washout of 2-APB resulted in a return of the current to a value not significantly different from the pre-2-APB level. Inhibition of the current was associated with a depolarisation of the reversal potential by 35.4 ± 5.5 mV (n=8). To exclude any possibility of a contribution of CRAC entry to the block observed by application of 2-APB, we repeated the experiments of Figure 6 in the absence of extracellular Ca^{2+} with identical block of the current by 2-APB (data not shown). Analysis of the whole cell IV relationships during 2-APB application provided no indication of voltage dependence of the 2-APB block.

The inhibitory sensitivity of KCa3.1 to block by 2-APB was determined and is presented in Figure 6D. The magnitude of the whole cell current at 0 mV, extracted from voltage ramps applied every second, was normalised to the magnitude of the current in the absence of 2-APB and fit to the Hill equation described in Materials and Methods. The solid line denotes the best fit of the data with $K_{1/2}$ = 14.2 μM, n = 1.8 and *Baseline* = 0.05 (n=4 to 8 cells for each data point).

3.5. Inhibition by 2-APB of KCa3.1 single channel open probability

To further substantiate the direct inhibition of KCa3.1 by 2-APB, the effects of this agent on single channel activity were investigated in the excised, inside out patch clamp configuration. Channel activity attributable to KCa3.1 was confirmed using the Ca^{2+} dependence of the activity, the magnitude of the unitary current at 0 mV holding potential, a negative reversal potential and the open channel kinetics, in accordance with our previous single channel characterisation of the charybdotoxin and TRAM-34-sensitive channel in HEL

cells [14,15]. Figure 7A shows the single channel activity recorded in a representative excised patch at a holding potential of 0 mV. The pipette contained standard extracellular NaCl solution identical to that used in the whole cell experiments presented earlier while the cytosolic face of the patch was superfused with KCl-based extracellular solution having a free Ca^{2+} concentration of 5 μM and a free Mg^{2+} concentration of 5 mM (see Materials and Methods). The Ca^{2+} dependence of the channel activity was first determined by superfusing the patch with a KCl-based solution having a free [Ca^{2+}] of 50 nM. This solution resulted in complete cessation of channel activity (data not shown). In addition, the channel displayed a highly negative reversal potential consistent with a strongly selective K^+ channel (data not shown). Application of 75 μM 2-APB to the cytosolic face of the patch was associated with a marked reduction in channel activity that was at least partially reversible upon wash-off. Representative channel activity at the indicated times are shown at higher temporal resolution in Panel A. To quantify the extent of the block of channel activity we have determined the NP_O value; the product of the channel number and the open channel probability, in the absence and presence of 2-APB. All-points-amplitude histograms were constructed from segments of the trace immediately before and during peak 2-APB block. The data were fit to multiple Gaussian distributions and NP_O calculated as described in Materials and Methods. The results for the experiment shown in Figure 7A are shown in Panel B. In the absence of 2-APB NP_O was 0.76. This has reduced to 0.04 in the presence of 2-APB. The results of 2-APB application in 8 independent experiments is shown in Panel C. To take into account the variability in channel number in the different patches, NP_O in the presence of 2-APB was normalised to that measured in its absence. In the presence of 75 μM 2-APB, NP_O was significantly reduced from 1 to 0.09 ± 0.02 ($p \leq 0.05$, n=8). Wash-off of 2-APB was accompanied by variable degrees of recovery of the channel activity as indicated by the large SEM.

3.6. Modulation by 2-APB of the single channel open time distribution of KCa3.1

A close inspection of the residual channel activity observed during exposure to 2-APB suggested that the opening events were of shorter duration than control opening events (see Figure 7A; higher temporal resolution channel activity). We have undertaken a simplified kinetic analysis to quantify the mean open times in the absence and presence of 2-APB. Open time distributions in the absence and presence of 2-APB were created for experiments in which only a single channel was present. The duration of channel openings were determined using a 50% threshold crossing method (see Materials and Methods). Representative analyses in the absence and presence of 2-APB in a single patch are shown in Figure 8A and B. In this experiment the mean open time (*To*) was calculated to be 6.7 ms in the absence of 2-APB (Panel A) and 2.8 ms in its presence (Panel B). As a result of the filter frequency used in the experiments and the need to filter post acquisition to reduce detection of false opening events associated with the signal to noise characteristics of the recording, brief openings are under-estimated in the distributions. This is particularly so in the presence of 2-APB where openings are much briefer. As such, our calculated mean open times should be considered as over-estimates. In spite of this caveat we found that the mean open time in the presence of 2-APB was significantly reduced by 52.8 ± 3.1 % from a value of 5.3 ± 0.7 ms in the absence of 2-APB to 2.5 ± 0.2 ms in its presence ($p \leq 0.05$, n=5) (Panel C).

4. Discussion

The present experiments in HEL cells document an absolute requirement for a hyperpolarised membrane potential for the onset activation of KCa3.1 leading to the augmented Ca^{2+} entry driven by a secondary hyperpolarisation. Additionally, our results highlight significant direct inhibition of the Ca^{2+}-activated K^+ channel KCa3.1 by the

established CRAC channel blocker 2-APB.

The importance of KCa3.1 in augmenting Ca^{2+} entry is well established in non-excitable cells [33,34,35] and the importance of KCa3.1 in augmenting Ca^{2+} entry in HEL has been previously proposed [23]. However, the physiological relevance of this mechanism in HEL cells was uncertain since the authors reported that KCa3.1 was not endogenously active. Our present data, and previous work from our laboratory [14,15], have demonstrated the constitutive expression of KCa3.1 and the present data strongly reinforces the physiological importance of this channel in the optimisation of Ca^{2+} entry mediated by depletion of endosomal Ca^{2+} stores. In contrast to previous investigations of the importance of KCa3.1 in augmenting CRAC-mediated Ca^{2+} entry, the focus of our investigations centered upon the onset activation of this channel and the importance of membrane potential in ensuring adequate Ca^{2+} entry for initiate of KCa3.1 channel activation. We have found that in intact HEL cells, depolarisation to 0 mV was accompanied by a fall in free Ca^{2+} to a value not expected to activate KCa3.1 [23,28,29] (Figure 1D). We have also shown using whole cell patch clamp that during activation of CRAC entry, a membrane potential of 0 mV is insufficient to elevate sub membranous free Ca^{2+} to levels required for KCa3.1 activation. Thus, a hyperpolarised resting membrane potential is an absolute requirement for onset activation of KCa3.1 in spite of the presence of a large inward Ca^{2+} gradient.

4.1. Feed-forward control of Ca^{2+} entry by KCa3.1-mediated hyperpolarisation

The role of KCa3.1-mediated hyperpolarisation in the control of Ca^{2+} entry is easily described by a simple feed-forward mechanism. In this scheme, a sufficient resting membrane potential is required to support adequate Ca^{2+} entry leading to activation of KCa3.1, hyperpolarisation and augmented Ca^{2+} entry. In fact, the data presented in Figure

1C is consistent with such a simple model. In this experiment the thapsigargin-mediated changes in $[Ca^{2+}]_i$ were biphasic. An initial rise in $[Ca^{2+}]_i$ following addition of thapsigargin was followed by a secondary rise which may be attributable to activation of KCa3.1 leading to hyperpolarisation and augmented net Ca^{2+} entry. Consistent with this interpretation, the secondary rise in $[Ca^{2+}]_i$ was abolished by addition of charybdotoxin as evident in Figure 1B and C. We have also performed preliminary experiments in which membrane potential was recorded under whole cell current clamp while simultaneously monitoring $[Ca^{2+}]_i$ using fluo3 dialysed into the cell from the patch pipette. Like the intact cell suspension experiments of Figure 1, the rise in $[Ca^{2+}]_i$ was frequently biphasic with the secondary rise in $[Ca^{2+}]_i$ being associated with a pronounced hyperpolarisation (see supplemental Figure S3).

To more directly investigate the role of membrane potential in the CRAC-mediated initial activation of KCa3.1 we employed measurements of the KCa3.1 current under whole cell voltage clamp. As noted above, these experiments demonstrate the absolute requirement for a negative potential for KCa3.1 activation. However, voltage clamp investigations of a feed-forward membrane potential mechanism regulating Ca^{2+} entry have a serious potential limitation. Voltage clamp effectively removes the feed-forward mechanism, since voltage is not allowed to change with any changes in $[Ca^{2+}]_i$. We have used the lack of detection of a measureable KCa3.1 current as evidence that the obligatory hyperpolarisation required to initiate the feed-forward process would not be evoked. To ensure that our ability to detect changes in KCa3.1 does not underlie our finding of a requirement for hyperpolarisation, we also undertook current clamp experiments. Under current clamp, membrane potential is free to change in response to even modest changes in $[Ca^{2+}]_i$ should they activate levels of KCa3.1 below our level of detection sensitivity in voltage clamp. Experiments such as those

presented in Figure 4B concur that at 0 mV, insufficient Ca^{2+} entry exists to support activation of KCa3.1 and subsequent hyperpolarisation; a surprising result considering the sustained inward chemical gradient for Ca^{2+}. Additionally, under current clamp, we observed a subset of cells that did not hyperpolarise in response to Ca^{2+} reintroduction after activation of the CRAC pathway (Figure 3B). Consistent with this arising from insufficient Ca^{2+} entry, hyperpolarisation mediated by current injection gave rise to a secondary hyperpolarisation that was sustained after termination of the injection current. We propose that this arises as a result of the augmented Ca^{2+} entry during current injection and the initiation of the feed-forward influence of voltage on secondary Ca^{2+} entry.

The temporal changes in membrane potential recorded under current clamp also support the existence of a feed-forward mechanism controlling Ca^{2+} entry. The hyperpolarisation observed during Ca^{2+} reintroduction frequently showed an initial hyperpolarising phase that gradually increased leading to a rapid hyperpolarisation as can be seen in Figures 3A and 4B. The exact origin of the slower initial phase of hyperpolarisation is unclear. However, modest Ca^{2+} entry, sufficient to activate a small subset of KCa3.1 channels localised to Ca^{2+} entry channels could give rise to the secondary rapid phase of hyperpolarisation via the simple feed-forward mechanism proposed. The kinetics of the change in membrane potential are expected to be altered by the resting potential and hence the initial rate of change of $[Ca^{2+}]_i$. The membrane potential required to facilitate the required Ca^{2+} elevation necessary for activation of KCa3.1 will, however, be a function of the degree of CRAC channel expression and activation, and the effectiveness of Ca^{2+} extrusion mechanism. It is also important to bear in mind that the sensitivity of Ca^{2+} entry to membrane potential is a nonlinear relationship given the inward rectification of the CRAC pathway in HEL cells [22] and other cell types [2,4]. As a result, small changes in potential

may give rise to large changes in [Ca^{2+}].

4.2. Implications of 2-APB block of KCa3.1

It is well established that 2-APB is a blocker of the CRAC current [6,7,8]. However, the importance of membrane potential in the control of elevations in $[Ca^{2+}]_i$ may in part underlie the fall in $[Ca^{2+}]_i$ associated with 2-APB application in HEL and other cells types. 2-APB would be expected to modulate CRAC-mediated Ca^{2+}_i levels via block of the accompanying hyperpolarisation in cells types where KCa3.1 plays an important role in the feed-forward regulation of Ca^{2+} entry. Such a proposal requires that 2-APB sufficiently blocks KCa3.1 to give rise to a reversal of the hyperpolarisation. In cells with modest depolarising conductances, potent block of KCa3.1 may be required. Our data presented in Figure 1B and C demonstrates the influence of block of KCa3.1 by charybdotoxin on $[Ca^{2+}]_i$. We also found an approximately 35 mV depolarising shift in the reversal potential in the presence of 75 μM 2-APB indicating that this concentration sufficiently inhibits KCa3.1, thereby reducing the driving force for Ca^{2+} entry. In fact, the dose response relationship presented in Figure 6D indicates that lower concentrations of 2-APB are expected to give similar effects.

Multiple reports in the literature have ascribed the fall in free Ca^{2+}_i and/or the decline in KCa3.1 current observed following application of 2-APB exclusively to its inhibitory effect on SOC/CRAC entry. Gao and co-workers [33] have demonstrated the importance of KCa3.1 in augmenting Ca^{2+} entry in human macrophages with the authors demonstrating a significant hyperpolarisation driven by this channel during activation of the CRAC entry pathway following UTP addition. Additionally, the authors demonstrate the importance of the charybdotoxin-sensitive KCa3.1 current in the maintenance of elevated steady-state

$[Ca^{2+}]_i$. However, the decline in free Ca^{2+}_i and the reversal of the KCa3.1-mediated hyperpolarisation observed following 50 μM 2-APB addition was ascribed exclusively to block of the CRAC pathway. Given our finding of direct block of the hyperpolarising current by this concentration of 2-APB, the mechanism of block by 2-APB of Ca^{2+} entry and the role of direct membrane potential modulation by 2-APB in human macrophages remains unclear. A similar conclusion can be drawn from experiments performed in rat microglial cells [29]. The authors demonstrate the presence of KCa3.1 and highlight its role in augmenting changes in $[Ca^{2+}]_i$ mediated by UTP. Again, the mechanism of block of Ca^{2+} entry and KCa3.1 currents measured directly under whole cell patch clamp conditions was ascribed exclusively to 2-APB (50 μM) block of Ca^{2+} entry. It remains to be determined if, like in HEL cells, 2-APB may contribute to Ca^{2+} signaling via direct block of KCa3.1 in other cells types.

In addition to our present results with 2-APB, the CRAC channel blocker BTP2 [36,37], a 3,5-bistrifluoromethyl pyrazole derivative, has also been implicated in control of Ca^{2+} signaling via direct modulation of membrane potential. However, in contrast to direct inhibition of a hyperpolarising effect, as we describe for 2-APB, BTP2 has been proposed to directly activate TRPM4, a depolarising conductance [38], at a concentration lower than that required to inhibit CRAC currents [37]. It is the subsequent depolarisation that has been proposed to underlie the inhibitory effect of BTP2 on Ca^{2+} influx and interleukin-2 production in Jurkat cells when used at low concentrations [37].

4.3. Promiscuous and complex modulation of ion transport processes by 2-APB

In addition to block of the CRAC channel, 2-APB is also known to block numerous ion transport processes of diverse function. These include block of endosomal Ca^{2+} pumps

[9], voltage-gated K^+ channels [10], the non-selective cation channel TRPM7 [11] and a Mg^{2+}-inhibited K^+ conductance described in HEL cells [12]. In spite of these documents actions, 2-APB block of Ca^{2+} elevations is still used as evidence of SOC/CRAC entry involvement. Our data not only highlight the inhibitory influence of 2-APB on KCa3.1 but provides an experimental framework whereby block of this channel can give rise to a decline in free Ca^{2+} levels mediated by CRAC entry without direct inhibition of the CRAC pathway.

The site of block of KCa3.1 by 2-APB is unclear. In the majority of our experiments 2-APB was added to the extracellular solution, giving rise to a rapid and potent inhibition of both the elevation in $[Ca^{2+}]_i$ mediated by thapsigargin and the whole cell KCa3.1 current accompanying whole cell dialysis with solutions containing high free Ca^{2+}. However, application of 2-APB to the cytosolic face of excised patches also resulted in a reduction in open channel probability and a decline in the mean open time of the residual channel activity. Interestingly, these effects seems to develop with an apparently longer time course. However, the kinetics of the inhibition were not studied in detail as a result of the limitations of our solution exchange procedures. Given the membrane permeability of 2-APB it is difficult to conclude whether the site of action is extracellular or intracellular. An extracellular site of action may account for less than 100% inhibition of the single channel open probability since diffusion across the membrane may give rise to a lower concentration at the extracellular face and a slower development of channel inhibition.

The mode or modes of action of 2-APB modulation of ion channels are complex. At high concentrations it blocks CRAC current activation [6,7,8] while at low concentrations it has been reported to augment CRAC currents in Jurkat cells [7]. However, the potentiating effect of low doses of 2-APB appears to be cell type specific [6,7,8]. High concentrations of 2-APB are also known to activate TRPV channels [39,40] while additional work has shown that at high concentrations this agent activates Orai3 channel homologues without a need for

Ca^{2+}-store depletion and presumably STIM1 engagement [41,42,43], giving rise to a nonselective cation current displaying both inward and outward rectification; a current clearly distinct from the highly Ca^{2+} selective CRAC current.

While 75 μM 2-APB markedly inhibits KCa3.1, lower doses reported to block the CRAC pathway also significantly inhibit the channel (Figure 6D) and blocked the CRAC entry pathway (see supplemental data Figure S4). Our estimated concentration yielding half inhibition of KCa3.1 is 14.2 μM. Inhibition of the CRAC current has been reported to have a half inhibition concentration of 5.5 μM in RBL cells [8] and 9.6 μM in Jurkat cells [7]. Thus, 2-APB is slightly more potent at blocking CRAC currents than it is at blocking KCa3.1 currents. However, at concentrations typically used in experiments designed to abolish Ca^{2+} entry mediated by CRAC and SOCE [29,33,44], KCa3.1 also undergoes near complete inhibition.

Like the complex effects of low doses of 2-APB on the modulation of the CRAC pathway in Jurkat cells [7], low doses caused somewhat confusing results in a small number of cells during investigations of inhibition of KCa3.1. In some experiments 5 μM 2-APB caused an inhibition of KCa3.1 followed by a potentiation during application or a potentiation following removal of the drug. However, this effect was inconsistent. As a result, for the construction of the dose response relationship presented in Figure 6D the data for 5 μM 2-APB was taken from experiments in which there was no significant modulation of the current during or after wash-off of 2-APB. The origin of this low dose effect is unclear. On one hand it may be indicative of complex interactions of low doses of 2-APB similar to those reported for CRAC currents [7]. Alternatively, the complex changes in KCa3.1 current observed in some experiments may arise from 2-APB-independent modulation of the channel by additional factors. The lack of consistency of this effect makes investigations of the phenomena difficult.

4.4. Importance of the resting membrane potential in cells of leukemic origin

The importance of ion channels in augmenting the Ca^{2+} driving force is well established in non-excitable cells. Numerous ion channels such as the voltage-dependent K^+ channel Kv1.3, [45], the intermediate and small conductance Ca^{2+}-activated K^+ channels including KCa3.1 [45,46,47,48] and a swelling-induced chloride conductance [49,50] have all been proposed to augment Ca^{2+} entry via their ability to hyperpolarise the membrane potential.

Our demonstration that 0 mV is unable to support sufficient Ca^{2+} entry for activation of KCa3.1 in HEL cells is, in our mind, surprising given the large residual chemical gradient. However, this is accounted for by the inwardly rectifying nature of the CRAC pathway as discussed above. The absolute requirement for a hyperpolarised potential has important implications for Ca^{2+} signaling in leukemic cells. Kapural and coworkers [51] have demonstrated suppression of conventional voltage-gated K^+ channel function and membrane depolarisation in megakaryocytes from patients with myelogenous leukemia. The authors also documented the absence of this channel in the leukemic cell lines HEL and CHRF-288-11, an observation substantiated by work from our laboratory [12 and the present study]. In spite of the absence of delayed rectifier type channel activity and any other conventional K^+ channel activity, we found that both HEL and CHRF-288-11 cells displayed a negative membrane potential [12]. We have previously reported that the conductance setting this negative resting potential was inhibited by elevated free Mg^{2+}_i but that the channel was active at physiological free Mg^{2+} concentrations giving rise to our designation of this as a Mg^{2+} inhibited potassium (MIP) current [12]. Importantly, we have reported that HEL cells display a negative resting potential under conditions that support activation of the non-

selective cation channel TRPM7 [12] which has a reversal potential near 0 mV given its non-selective cation permeability [52,53]. We propose that in the face of constitutive activation of TRPM7, the MIP conductance plays a critical role in ensuring a sufficient hyperpolarised resting potential to support onset activation of KCa3.1 during CRAC channel activation.

5. **Conclusions**

Our results highlight the absolute requirement for membrane hyperpolarisation for adequate Ca^{2+} entry leading to KCa3.1 activation. These results highlight the critical importance of the hyperpolarising MIP conductance described in leukemic cell lines [12] for the initiation of optimum Ca^{2+} signaling events. Additionally, the present results demonstrate inhibition of KCa3.1 by 2-APB and highlight the need for caution when interpreting the site of action of 2-APB in cells expressing KCa3.1.

Figure Legends

Fig. 1. Effect of 2-APB and membrane potential on thapsigargin-mediated elevations in $[Ca^{2+}]_i$ in cuvette suspensions of HEL cells. (A-C) Fluo3 loaded cells were suspended in NaCl or NMDGCl-based extracellular solutions containing 1 mM Ca^{2+}. Where indicated, 200 nM thapsigargin, 75 μM 2-APB, 200 nM charybdotoxin (CTX) and 200 nM gramicidin were added. All experiments were performed at 20-22^{o}C. (D) Summary of the effect of changes in membrane potential induced by charybdotoxin and gramicidin addition in NaCl or NMDGCl-based solutions. &, #, and *, significantly different at $p \leq 0.05$, n=3.

Fig. 2. Effect of holding potential on the magnitude of the KCa3.1 current stimulated by CRAC entry. A cell was superfused with standard extracellular NaCl-based solution

containing 1 mM Ca^{2+} and whole cell patched using a low Ca^{2+}, KCl-based pipette solution. The indicated 200 ms voltage ramps from -100 to +100 mV were administered every 3 seconds from a holding potential of -80 or 0 mV. (A) The magnitude of the whole cell ramp current at 0 mV was extracted from individual ramps and plotted as a function of time. Where indicated the cell was superfused with NaCl-based solution containing 1 μM thapsigargin. Holding potential (HP) and extracellular Ca^{2+} were changed as indicated. (B) representative ramp currents applied from holding potentials of -80 or 0 mV. The traces labeled 1 through 4 are the ramp currents at the indicated time points presented in Panel A. (C) Summary of the effect of holding potential on the magnitude of the KCa3.1 current stimulated by CRAC entry. The ramp current at 0 mV has been normalised to the ramp current at 0 mV recorded at a holding potential (HP) of -80 mV during addition of 1 μM thapsigargin. & and *, significantly different at $p \leq 0.05$, n=9.

Fig. 3. Current clamp measurements of membrane hyperpolarisation mediated by activation of KCa3.1. Cells were whole cell patched and membrane potential monitored under current clamp. The cells were superfused with 200 nM thapsigargin in Ca^{2+}-free Na^{+} solution as noted. Where indicated the solution was changed to Na^{+} solution containing 1 mM Ca^{2+}. Where indicated in Panel B current was transiently injected to hyperpolarise the cell.

Fig. 4. Effect of holding potential on the magnitude of the KCa3.1 conductance stimulated by CRAC entry in the absence of intracellular EGTA. A cell was superfused with standard extracellular NaCl-based solution containing 1 mM Ca^{2+} and whole cell patched using a low Ca^{2+}, KCl-based pipette solution devoid of added EGTA. (A) Representative ramp currents applied from holding potentials of -80 or 0 mV. 200 ms voltage ramps from -100 to +100 mV from the indicated holding potentials were administered every 3 seconds. (B) The same

cell used in the voltage clamp experiments of Panel A was placed in current clamp after inhibition of KCa3.1 mediated by a holding potential of 0 mV. The start of the record in Panel B shows the transition from voltage clamp (0 mV holding potential) to current clamp. The second section of Panel B shows a similar transition from voltage clamp to current clamp with the exception that a small positive injection current (approximately 11 pA) was quickly applied to depolarise the cell to approximately 0 mV. Where indicated the injection current was turned off.

Fig. 5. Effect of holding potential on the magnitude of the KCa3.1 current activated by 5 μM cytosolic Ca^{2+}. A cell was superfused with standard extracellular NaCl-based solution containing 1 mM Ca^{2+} and whole cell patched using a KCl-based pipette solution with a free Ca^{2+} concentration of 5 μM. 200 ms voltage ramps from -100 to +100 mV were administered every 3 seconds from a holding potential of -80 or 0 mV. (A) The magnitude of the whole cell ramp current at 0 mV was extracted from individual ramps and plotted as a function of time. Holding potential (HP) and extracellular Ca^{2+} were changed as indicated. (B) Representative ramp currents applied from holding potentials of -80 or 0 mV. The traces labeled 1 through 3 are the ramp currents at the indicated time points presented in Panel A.

Fig. 6. Block of whole cell KCa3.1 current by 2-APB. A cell was superfused with standard extracellular NaCl-based solution containing 1 mM Ca^{2+} and whole cell patched using a KCl-based pipette solution with a free Ca^{2+} concentration of 5 μM. 200 ms voltage ramps from -100 to +100 mV were administered every 3 seconds from a holding potential of -80 or 0 mV. (A) The magnitude of the whole cell ramp current at 0 mV was extracted from individual ramps and plotted as a function of time. Holding potential (HP) was changed and 75 μM 2-APB added as indicated. (B) Representative ramp currents in the absence and

presence of 2-APB, The traces labeled 1 and 2 are the ramp currents at the indicated time points presented in Panel A. (C) Summary of the effect of changes in holding potential and addition of 75 μM 2-APB on the ramp current at 0 mV. The ramp currents at 0 mV were normalised the magnitude of the current at a -80 mV holding potential (HP). @,* and &, significantly different at $p \leq 0.05$, n=8. (D) Degree of KCa3.1 inhibition by 2-APB. The current at 0 mV in the presence of 2-APB was normalised to the current in its absence. The solid line is the best fit to the Hill equation described in Materials and Methods with $K_{1/2}$ = 14.2 μM, n = 1.8 and *Baseline* = 0.05. n=4 to 8 for each data point.

Fig. 7. Block by 2-APB of KCa3.1 single channel activity. Excised patch recording of KCa3.1 activity. The pipette solution was the 1 mM Ca^{2+}, NaCl-based extracellular solution used in Fig. 2, 4 and 5. The cytosolic face of the patch was superfused with a KCl-based , 5 μM free Ca^{2+} solution identical to that used as the whole cell pipette solution used in Figs. 4 and 5. (A) Single channel activity at 0 mV holding potential in a patch containing 2 apparent channels. Where indicated, the patch was superfused with solution containing 75 μM 2-APB. Higher temporal resolutions segments of channel activity are shown in the lower traces. The closed state, c, and open channel current levels are denoted on the left of the traces. (B) All-points-amplitude histograms in the absence and presence of 2-APB. Identical record lengths immediately before and during peak 2-APB inhibition were used to construct the histograms. Histograms were fit to the sum of multiple Gaussian distributions and NPo calculated as described in Materials and Methods. i is the number of single channel current levels. (C) Summary of the effect of 75 μM 2-APB inhibition of the open channel probability of KCa3.1. NPo was normalised to the value in the absence of 2-APB (Pre-2-APB). * and &, significantly different at $p \leq 0.05$, n=8.

Fig. 8. Effect of 2-APB on single channel mean open times. Open time distributions were determined for identical segment lengths in the absence and presence of 75 μM 2-APB in patches containing a single channel as described in Materials and Methods. (A). Open time distributions in a representative patch. *To*, the mean open time was calculated as the mean of all open events of all durations. (B) Summary of the effect of 75 μM 2-APB on the mean open time. *, significantly different at $p \leq 0.05$, n=5.

Supplemental Fig. S1. Comparison of the initial rise in $[Ca^{2+}]_i$ mediated by thapsigargin addition in the presence and absence of 1 mM extracellular Ca^{2+}. Fluo3 loaded cell suspensions were added to a cuvette under continual stirring and 200 nM thapsigargin added were indicated. The data is presented as raw photomultiplier tube output. The traces have been scaled to ensure identical F_{max} to F_{Mn} voltage ranges thus ensuring identical dynamic fluorescence ranges for each experiment. For ease of comparison of the magnitude and rate of change in fluorescence the traces have been aligned.

Supplemental Fig. S2. Current clamp measurements of membrane hyperpolarisation mediated by activation of KCa3.1. (A) A cell was whole cell patched and membrane potential monitored under current clamp. The cell was superfused with 200 nM thapsigargin in Ca^{2+}-containing Na^+ solution as noted. Where indicated Ca^{2+} was removed or added to the Na^+ solution.

Supplemental Fig. S3. Simultaneous measurement of fluo3 fluorescence and membrane potential under whole cell current clamp. A single cell was whole cell patched with a low Ca^{2+}, KCl-based solution supplemented with 50 μM fluo3 free salt. The solution is identical to that used in our thapsigargin whole cell patch clamp experiments with the exception that

50 μM EGTA was replaced with 50 μM fluo3. Membrane potential was recorded under current clamp and fluo3 fluorescence monitored using a photomultiplier-based fluorescence system attached to the side-port of the microscope. Fluo3 fluorescence is reported as the raw photomultiplier tube output.

Supplemental Fig. S4. Effect of 25 μM 2-APB on thapsigargin-mediated elevations in $[Ca^{2+}]_i$ in cuvette suspensions of HEL cells. Fluo3 loaded cells were suspended in NaCl solution identical to that used in Figure 1A. Where indicated, 100 nM thapsigargin and 25 μM 2-APB were added. The experiment was performed at 20-22^{o}C.

Appendix A. Supplemental data

This article contains supplemental data.

Acknowledgement

The authors thank Colin Stoneking for helpful discussions regarding the single channel kinetic analysis and for modifying the IGOR procedure used in this analysis.

References

1. J.W. Putney Jr., A model for receptor-regulated calcium entry, Cell Calcium 7 (1986) 1–12.

2. M. Hoth, R. Penner, Depletion of intracellular calcium stores activates a calcium current in mast cells, Nature 355 (1992) 353-355.

3. M.D. Cahalan, STIM-ulating store-operated Ca^{2+} entry, Nature Cell Biol. 11 (2009) 669-677.

4. A. Zweifach, R.S Lewis, Mitogen-regulated Ca current of T lymphocytes is activated by depletion of intracellular Ca^{2+} stores, Proc. Natl Acad. Sci. USA 90 (1993) 6295–6299.

5. A. Parekh, Store-operated CRAC channels: function in health and disease, Nat. Rev. Drug Discovery, 9 (2010) 399-410.

6. D. Bakowski, M.D Glitsch, A.B. Parekh, An examination of the secretion-like coupling model for the activation of the Ca^{2+} release-activated Ca^{2+} current I_{CRAC} in RBL-1 cells, J. Physiol. 532 (2001) 55–71.

7. M. Prakriya, R.S. Lewis, Potentiation and inhibition of Ca^{2+} release-activated Ca^{2+} channels by 2-aminoethyldiphenyl borate (2-APB) occurs independently of IP_3 receptors, J. Physiol. 536 (2001) 3–19.

8. T. Voets, J. Prenen , A. Fleig, R. Vennekens, H. Watanabe, J.G.J. Hoenderop, R.J.M. Bindels, G. Droogmans, R. Penner, B. Nilius B, CaT1 and the calcium release-activated calcium channel manifest distinct pore properties, J. Biol. Chem. 276 (2001) 47767– 47770.

9. L. Missiaen, G. Callewaert, H. De Smedt H, J.B. Parys, 2-Aminoethoxydiphenyl borate affects the inositol 1,4,5-trisphosphate receptor, the intracellular Ca^{2+} pump and the non-specific Ca^{2+} leak from the non-mitochondrial Ca2+ stores in permeabilized A7r5 cells, Cell Calcium 29 (2001) 11–116.

10. Y. Wang, M. Deshpande, R.Payne, 2-Aminoethoxydiphenyl borate inhibits phototransduction and blocks voltage-gated potassium channels in *Limulus* ventral photoreceptors, Cell Calcium 32: (2002) 209 –216.

11. M. Hermosura, M.K. Monteilh-Zoller, A.M. Scharenberg, R. Penner R, A. Fleig, Dissociation of the store-operated calcium current I_{CRAC} and the Mg-nucleotide-regulated metal ion current MagNuM, J. Physiol. 539 (2002) 445– 458.

12. M.J. Mason, C. Schaffner, R.A. Floto, Q.A. Teo, Constitutive expression of a Mg^{2+} inhibited K^+ current and a TRPM7-like current in human erythroleukemia cells, Am. J. Physiol. Cell Physiol. 302 (2012) C853-C867.

13. P. Martin, T. Papayannopoulou , HEL cells: a new human erythroleukemia cell line with spontaneous and induced globin expression, Science 216 (1982) 1233–1235.

14. C.J. Stoneking, O. Shivakumar, D. Nicholson Thomas, W.H. Colledge, M.J. Mason, Voltage dependence of the Ca^{2+}-activated K^+ channel $K_{Ca}3.1$ in human erythroleukemia cells, Am. J. Physiol. Cell. Physiol. 304 (2013) C858-C872.

15. C.J. Stoneking, M.J. Mason, Mg^{2+} modulation of the single channel properties of $K_{ca}3.1$ in human erythroleukemia cells, Pflügers Arch. 466 (2014)1529-1539.

16. K. Aoki, K. Kosakai, M. Yoshino, Monoaminergic modulation of the Na^+-activated K^+ channel in Kenyon cells isolated from the mushroom body of the cricket (*Gryllus bimaculatus*) brain, J. Neurophysiol. 100 (2008) 1211–1222.

17. A.A. Selyanko, J.K. Hadley, D.A. Brown, Properties of single M-type KCNQ2/KCNQ3 potassium channels expressed in mammalian cells, J. Physiol. 534 (2001) 15–24.

18. Y. Li, N. Gamper, M.S. Shapiro, Single-channel analysis of KCNQ K^+ channels reveals the mechanism of augmentation by cysteine-modifying reagents, J. Neurosci. 24 (2004) 5079–5090.

19. D. Colquhoun, Practical analysis of single channel records, in: D.C. Ogden (Ed.), Microelectrode techniques. The Plymouth workshop handbook, 2nd edn., The Company of Biologists Ltd., Cambridge, pp. 101–139.

20. E. Neher, Correction for liquid junction potentials in patch clamp experiments, Methods Enzymol .207 (1992) 123–131.

21. N.E. Evans, M.K.L. Forth, A.K. Simpson, M.J. Mason, Inhibition by calyculin A and okadaic acid of the Ca^{2+} release-activated Ca^{2+} entry pathway in rat basophilic leukemia cells: Evidence for regulation by type 1/2A serine/threonine phosphatase activity, BBA Biomembranes 1718 (2005) 32-43.

22. B. Somasundaram, M.J. Mason, M.P. Mahaut-Smith, Thrombin-dependent calcium signalling in single human erythroleukaemia cells, J. Physiol. 501 (1997) 485-495.

23. X. Lu, A. Fein, M.B. Feinstein, F.A. O'Rourke, Antisense knock out of the inositol 1,3,4,5-tetrakisphosphate receptor GAP1IP4BP in the human erythroleukemia cell line leads to the appearance of intermediate conductance K(Ca) channels that hyperpolarize the membrane and enhance calcium influx, J. Gen. Physiol. 113 (1999) 81-95.

24. O.S. Andersen, R.E. Koeppe II, Molecular determinants of channel function, Physiol. Rev. 72 (Suppl. 4) (1992) S89-S158.

25. S. Grinstein, J.D. Goetz, A. Rothstein, $^{22}Na^+$ fluxes through thymic lymphocytes: I. Na^+/Na^+ and Na^+/H^+ exchange through an amiloride-sensitive pathway, J. Gen. Physiol. 84 (1984) 565-584.

26. O. Wilson, I. Marriott, M.P. Mahaut-Smith, M.J. Mason, Isolation of a Ca^{2+} conductance activated by depletion of an intracellular Ca^{2+} pool in rat thymic lymphocytes,

J. Membr. Biol. 137 (1994) 159-168.

27. M.P. Mahaut-Smith, L.C. Schlichter, Ca^{2+}-activated K^+ channels in human B lymphocytes and rat thymocytes, J. Physiol. 415 (1989) 69-83.

28. M.P. Mahaut-Smith, M.J. Mason, Single channel recordings of Ca^{2+}-activated K^+ channels in rat lymphocytes: Activation by concanavalin A, J. Physiol. 439 (1991) 513-528.

29. R. Ferreira, L.C. Schlicter, Selective activation of KCa3.1 and CRAC channels by P_2Y_2 receptors promotes Ca^{2+} signaling, store refilling and migration of rat microglial cells, PLOS One 8 (2013) e62345-e62345.

30. M.P. Mahaut-Smith, J.F. Hussain, M.J. Mason, Depolarization-evoked Ca^{2+} release in a non-excitable cell, the rat megakaryocyte, J. Physiol. 515 (1999) 385–390.

31. M.J. Mason, M.P. Mahaut-Smith, Voltage-dependent Ca^{2+} release in rat megakaryocytes requires functional IP_3 receptors, J. Physiol. 533 (2001) 175–183.

32. M.J. Mason, M.P. Mahaut-Smith, Measurement and Manipulation of Intracellular [Ca^{2+}] in Single Platelets and Megakaryocytes, in: J.M. Gibbins, M.P. Mahaut-Smith (Ed.), Platelets and Megakaryocytes Volume 2: Perspectives and Techniques, Humana Press, USA, 2004, pp. 251-275.

33. Y.D. Gao, P.J. Hanley, S. Rinn, M. Zuzarte, J. Daut, Calcium-activated K^+ channel ($K_{Ca}3.1$) activity during Ca^{2+} store depletion and store-operated Ca^{2+} entry in human macrophages, Cell Calcium 48 (2010) 19-27.

34. S.M. Duffy, P. Berger, G. Cluse, W. Yang, S.J. Bolton, P. Bradding, The K^+ channel $iK_{CA}1$ potentiates Ca^{2+} influx and degranulation in human lung mast cells, J. Allergy Clin. Immunol. 114 (2004) 66-72.

35. R.S. Lewis, M.D. Cahalan, Potassium and calcium channels in lymphocytes, Annu. Rev. Immunol. 13 (1995) 623-653.

36. C. Zitt, B. Strauss, E.C. Schwarz, N. Spaeth, G. Rast, A. Hatzelmann, M. Hoth, Potent inhibition of Ca^{2+} release-activated Ca^{2+} channels and T-lymphocyte activation by the pyrazole derivative BTP2, J. Biol. Chem. 279 (2004) 12427-12437.

37. R. Takezawa, H. Cheng, A. Beck, J. Ishikawa, P. Launay, H. Kubota, J.-P. Kinet, A. Fleig, T. Yamada, R. Penner, A pyrazole derivative potently inhibits lymphocyte Ca^{2+} influx and cytokine production by facilitating transient receptor potential melastatin 4 channel activity, Mol. Pharmacol. 69 (2006)1413-1420.

38. P. Launay, A. Fleig, A., A.-L. Perraud, A.M. Scharenberg, R. Penner, R. J.-P. Kinet, TRPM4 is a Ca^{2+}-activated nonselective cation channel mediating cell membrane depolarization, Cell 109 (2002) 397-407.

39. H.Z. Hu, Q. Gu, C. Wang, C.K. Colton, J. Tang, M. Kinoshita-Kawada, L.-Y. Lee, J.D.

Wood, M.X. Zhu, 2-Aminoethoxydiphenyl borate is a common activator of TRPV1, TRPV2 and TRPV3, J. Biol. Chem. 279 (2004) 35741-35748.

40. M.K. Chung, H. Lee, A. Mizuno, M. Suzuki, M.J. Caterina, 2-Aminoethoxydiphenyl borate activates and sensitizes the heat-gated ion channel TRPV3, J. Neurosci. 24 (2004) 5177–5182.

41. W.I. DeHaven, J.T. Smyth, R.R. Boyles, G.S. Bird, J.W. Putney Jr, Complex actions of 2-aminoethyldiphenyl borate on store-operated calcium entry, J. Biol. Chem. 283 (2008) 19265-19273.

42 C. Peinelt, A. Lis, A. Beck, A. Fleig,, R. Penner, 2-Aminoethoxydiphenyl borate directly facilitates and indirectly inhibits STIM1-dependent gating of CRAC channels, J. Physiol. 586 (2008) 3061-3073.

43. S.L. Zhang,, J.A. Kozak, W. Jiang, A.V. Yeromin, J. Chen, Y. Yu, A. Penna, W. Shen, V. Chi, M.D. Cahalan, Store-dependent and -independent modes regulating Ca^{2+} release-activated Ca^{2+} channel activity of human Orai1 and Orai3, J. Biol. Chem. 283 (2008)17662-17671.

44. Y. Dobrydneva, P. Blackmore, 2-Aminoethoxydiphenyl borate directly inhibits store-operated calcium entry in human platelets, Mol. Pharmacol. 3 (2001) 541-552.

45. C.S. Lin, R.C. Boltz, J.T. Blake, M. Nguyen, A. Talento, P.A. Fischer, M.S. Springer, N.H. Sigal, R.S. Slaughter, M.L. Garcia, G.J. Kaczorowski, G.C. Koo, Voltage-gated potassium channels regulate calcium-dependent pathways involved in human T lymphocyte activation, J. Exp. Med. 177 (1993) 637-645.

46. B.S. Jensen, N. Odum, N.K. Jorgensen, P. Christophersen, S.-P. Olesen, Inhibition of T cell proliferation by selective block of Ca^{2+}-activated K^+ channels, Proc. Natl. Acad. Sci. USA 96 (1999) 10917-10921.

47. R. Desai, A. Peretz, H. Idelson, P. Lazarovici, B. Attali, Ca^{2+}-activated K^+ channels in human leukemic Jurkat T cells. Molecular cloning, biochemical and functional characterization, J. Biol. Chem. 275 (2000) 39954 -39963.

48. H. Wulff, M.J. Miller, W. Hansel, S. Grissmer, M.D. Cahalan, K.G. Chandy, Design of a potent and selective inhibitor of the intermediate-conductance Ca^{2+}-activated K^+ channel, IKCa1: a potential immunosuppressant, Proc. Natl. Acad. Sci. USA 97 (2000) 8151-8156.

49. R.S. Lewis, P.E. Ross, M.D. Cahalan, Chloride channels activated by osmotic stress in T lymphocytes, J. Gen. Physiol. 101 (1993) 801-826.

50. P.E. Ross, S.S. Garber, M.D. Cahalan, Membrane chloride conductance and capacitance in Jurkat T lymphocytes during osmotic swelling. Biophys. J. 66 (1994)169-178.

51 L. Kapural, M.B. Feinstein, F. O'Rourke, A. Fein, Suppression of the delayed rectifier type of voltage gated K43 outward current in megakaryocytes from patients with myelogenous leukemias, Blood 86 (1995)1043–1055.

52. M.J.S. Nadler, M.C. Hermosura, K. Inabe, A.L. Perraud, Q. Zhu, J. Stokes, T. Kusosaki, J.-P. Kinet, R. Penner, A.M. Scharenberg, A.F. Fleig, LTRPC7 is a Mg ATP-regulated divalent cation channel required for cell viability, Nature 411 (2001) 590-597.

53. L.W. Runnels. L. Yue, D.E. Clapham, TRP-PLIK, a bifunctional protein with kinase and ion channel activities, Science 291 (2001) 1043-1047.

Fig. 1

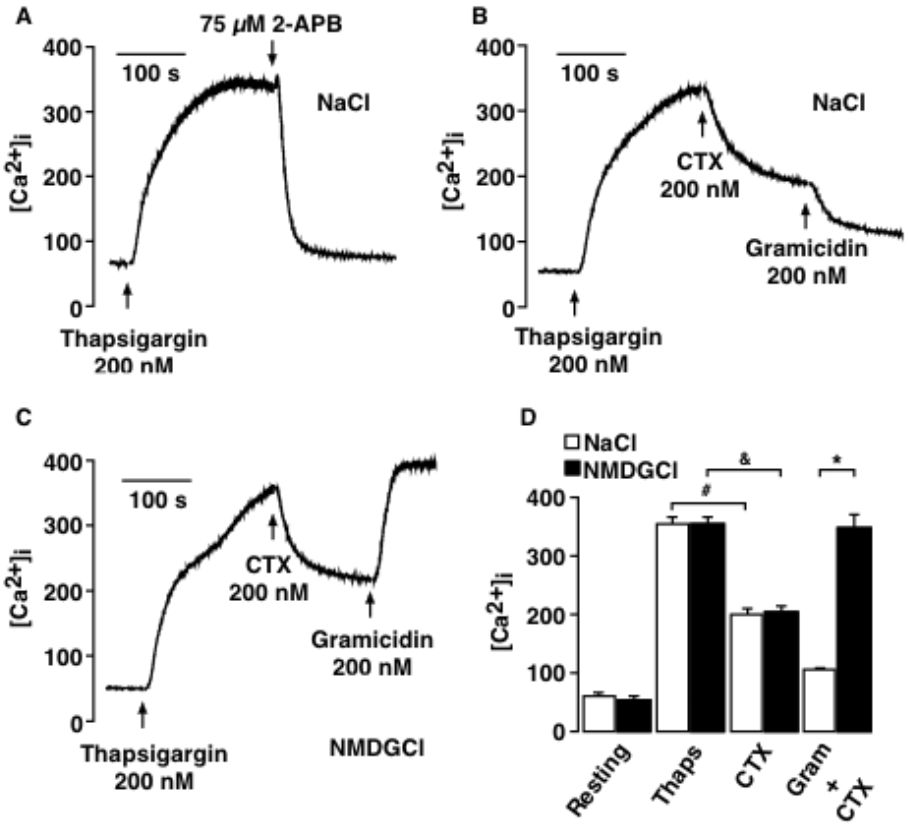
A
75 μM 2-APB
100 s
NaCl
[Ca2+]i
400
300
200
100
0
Thapsigargin
200 nM
B
100 s
NaCl
CTX
200 nM
Gramicidin
200 nM
Thapsigargin
200 nM
C
100 s
CTX
200 nM
Gramicidin
200 nM
Thapsigargin
200 nM
NMDGCl
D
NaCl
NMDGCl
&
*
#
Resting
Thaps
CTX
Gram + CTX

Fig. 2

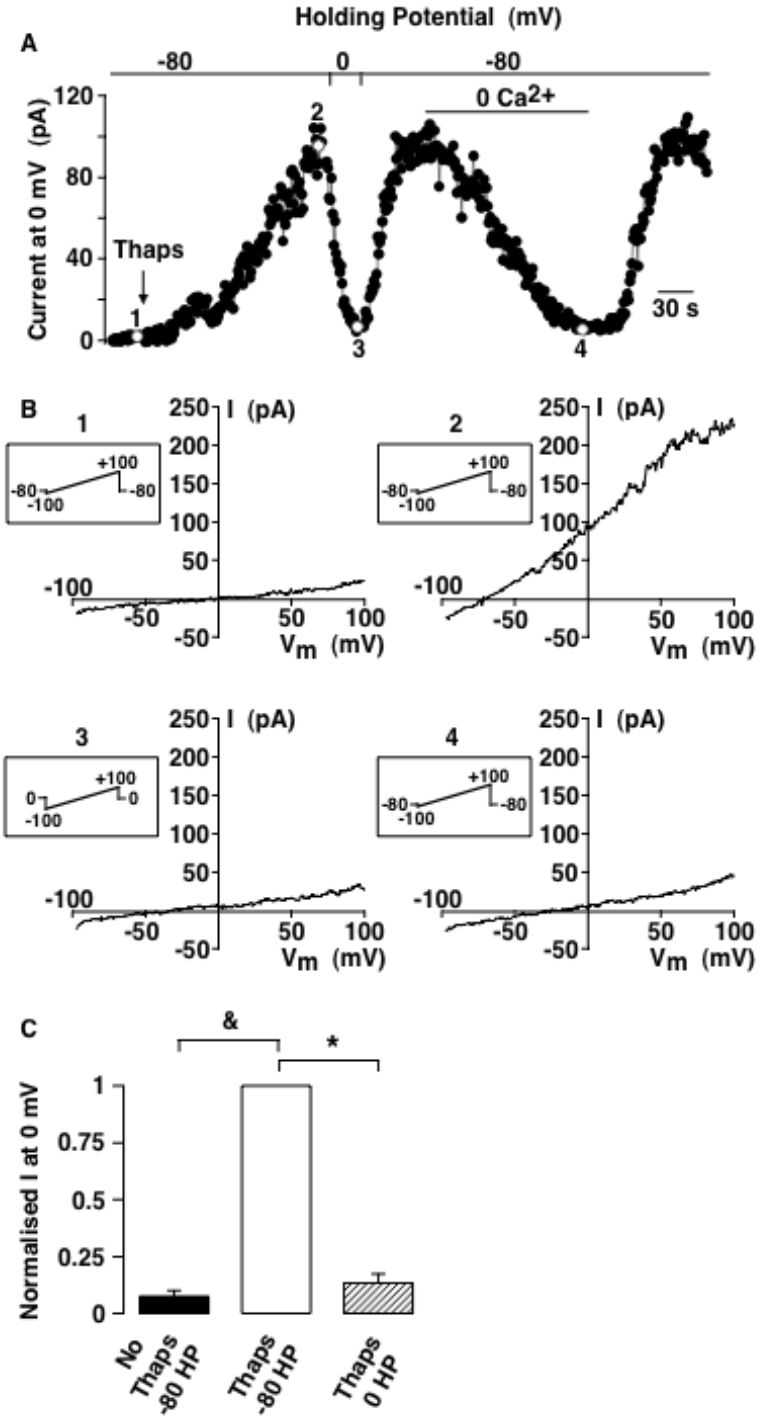
A
Holding Potential (mV)
-80
0
-80
0 Ca2+
Current at 0 mV (pA)
Thaps
30 s
B
1
2
3
4
I (pA)
Vm (mV)
C
Normalised I at 0 mV
No Thaps -80 HP
Thaps -80 HP
Thaps 0 HP
&
*

Fig. 3

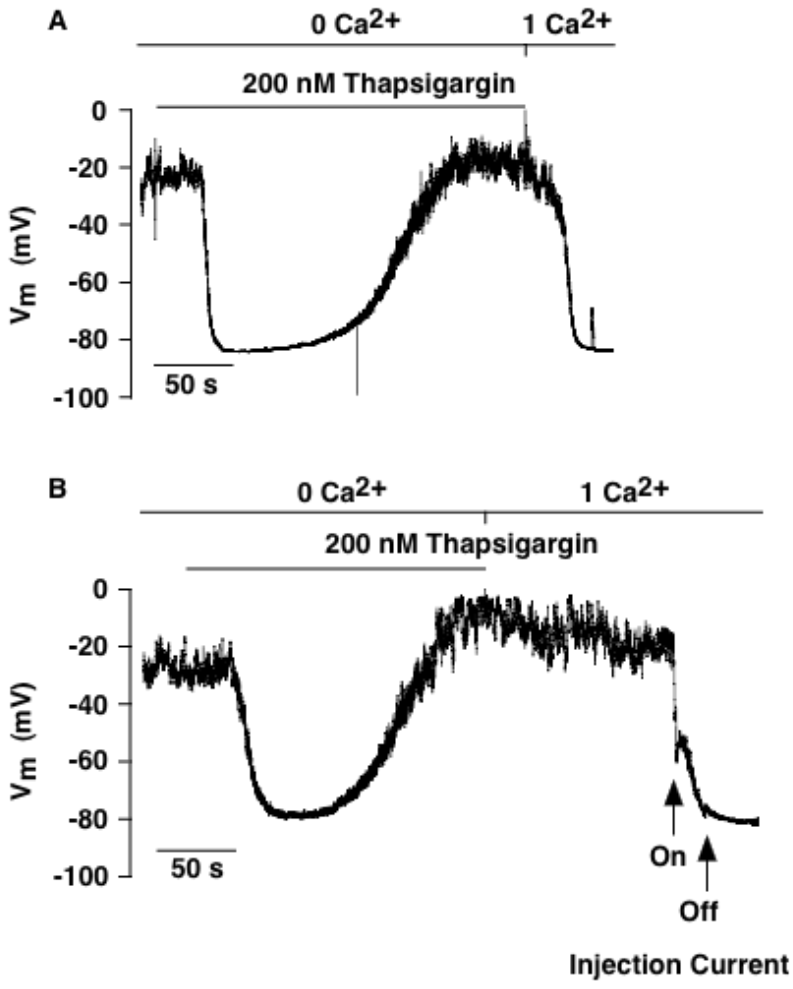
A
0 Ca2+
1 Ca2+
200 nM Thapsigargin
0
-20
-40
-60
-80
-100
Vm (mV)
50 s
B
0 Ca2+
1 Ca2+
200 nM Thapsigargin
0
-20
-40
-60
-80
-100
Vm (mV)
50 s
On
Off
Injection Current

Fig. 4

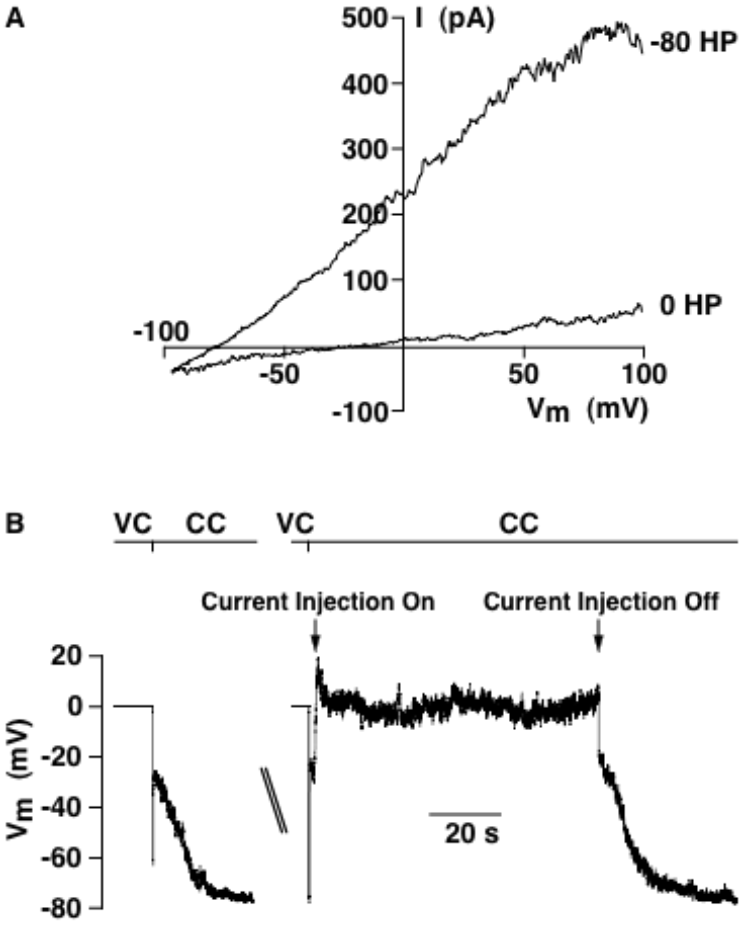
A
500
I (pA)
-80 HP
400
300
200
100
0 HP
-100
-50
50
100
-100
Vm (mV)
B
VC
CC
VC
CC
Current Injection On
Current Injection Off
20
0
-20
-40
-60
-80
Vm (mV)
20 s

Fig. 5

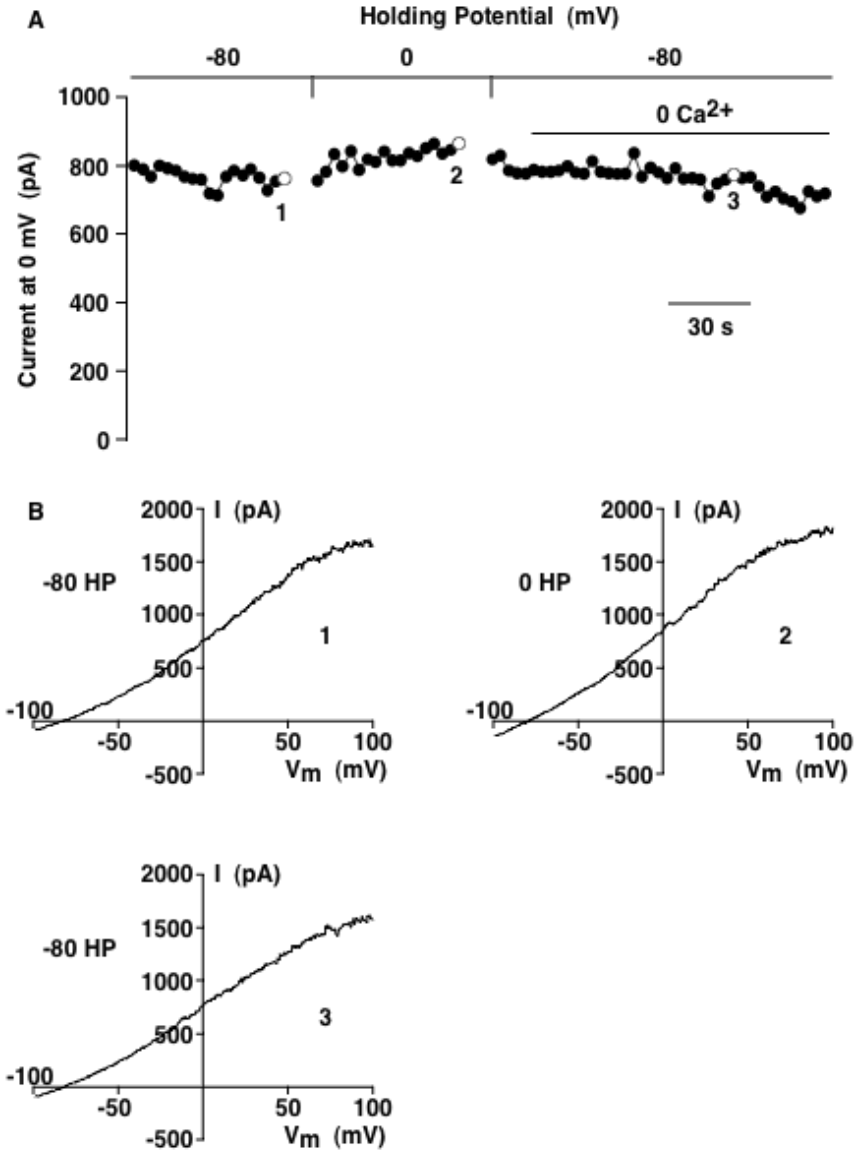
A
Holding Potential (mV)
-80
0
-80
0 Ca2+
Current at 0 mV (pA)
1000
800
600
400
200
0
1
2
3
30 s
B
I (pA)
-80 HP
0 HP
2000
1500
1000
500
-500
-100
-50
50
100
Vm (mV)

Fig. 6

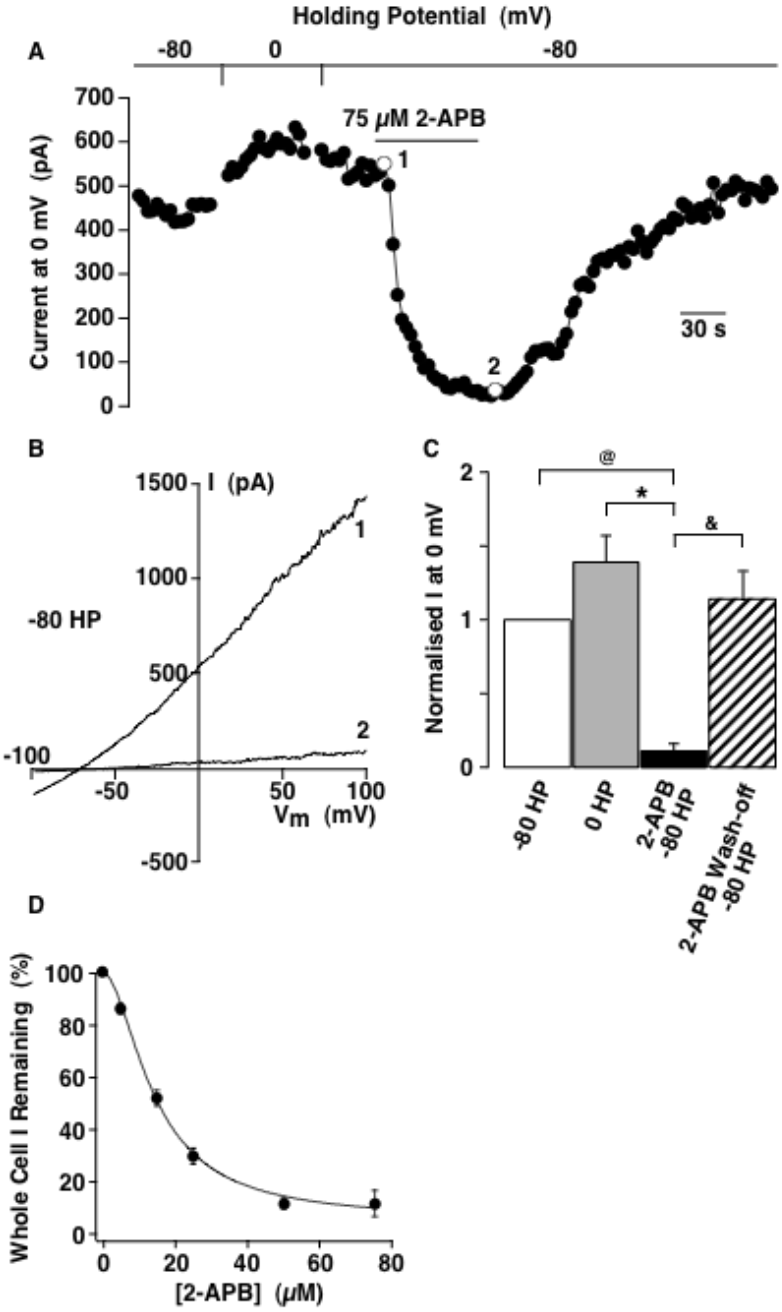
A
Holding Potential (mV)
-80
0
-80
75 μM 2-APB
1
2
30 s
Current at 0 mV (pA)
700
600
500
400
300
200
100
0
B
I (pA)
1500
1000
500
-500
-80 HP
-100
-50
50
100
Vm (mV)
1
2
C
Normalised I at 0 mV
2
1
0
@
*
&
-80 HP
0 HP
2-APB -80 HP
2-APB Wash-off -80 HP
D
Whole Cell I Remaining (%)
100
80
60
40
20
0
0
20
40
60
80
[2-APB] (μM)

Fig. 7

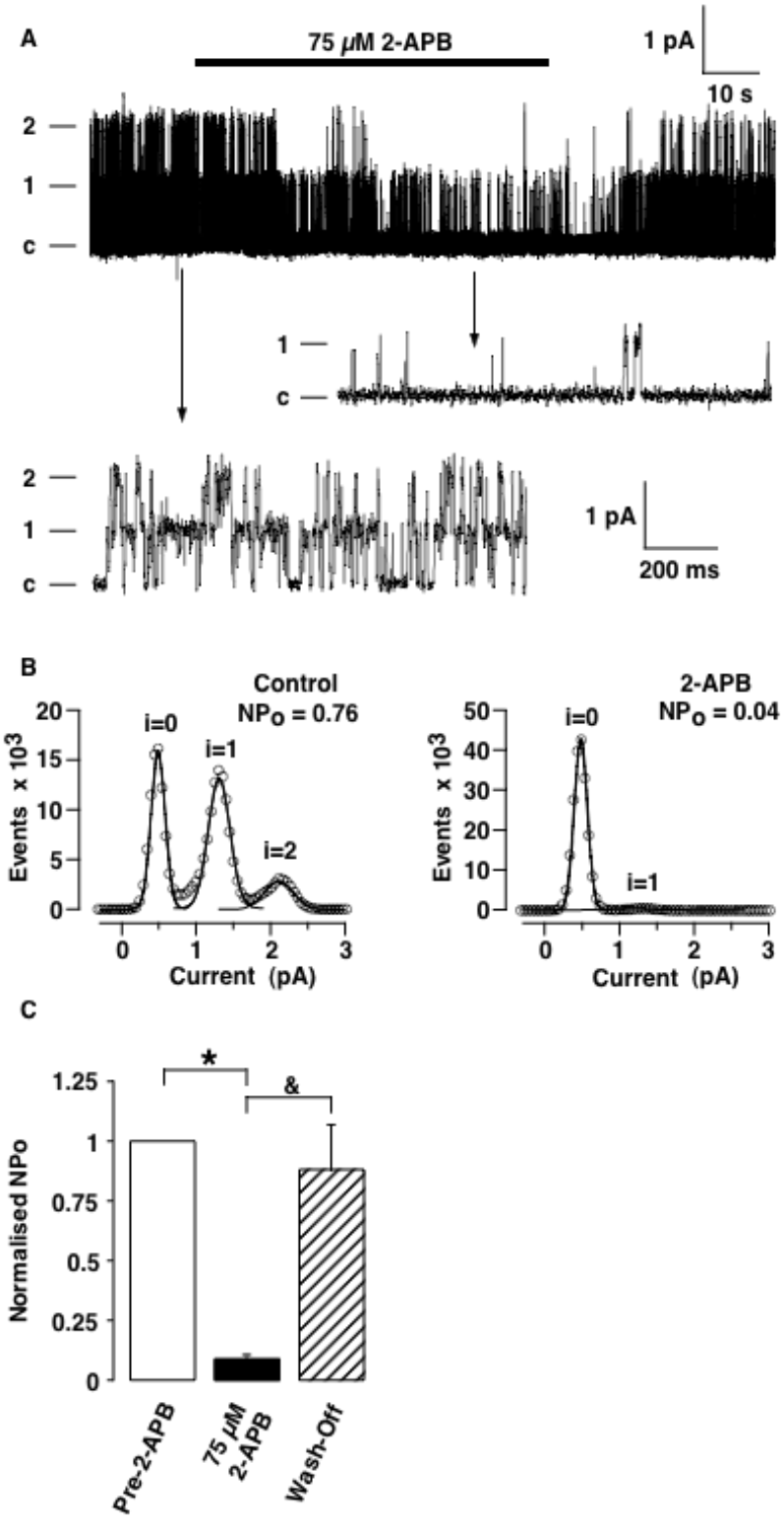
A
75 μM 2-APB
1 pA
10 s
2
1
c
1
c
2
1
c
1 pA
200 ms
B
Control
NPo = 0.76
i=0
i=1
i=2
Events x 10^3
Current (pA)
2-APB
NPo = 0.04
i=0
i=1
Events x 10^3
Current (pA)
C
*
&
Normalised NPo
Pre-2-APB
75 μM 2-APB
Wash-Off

Fig. 8

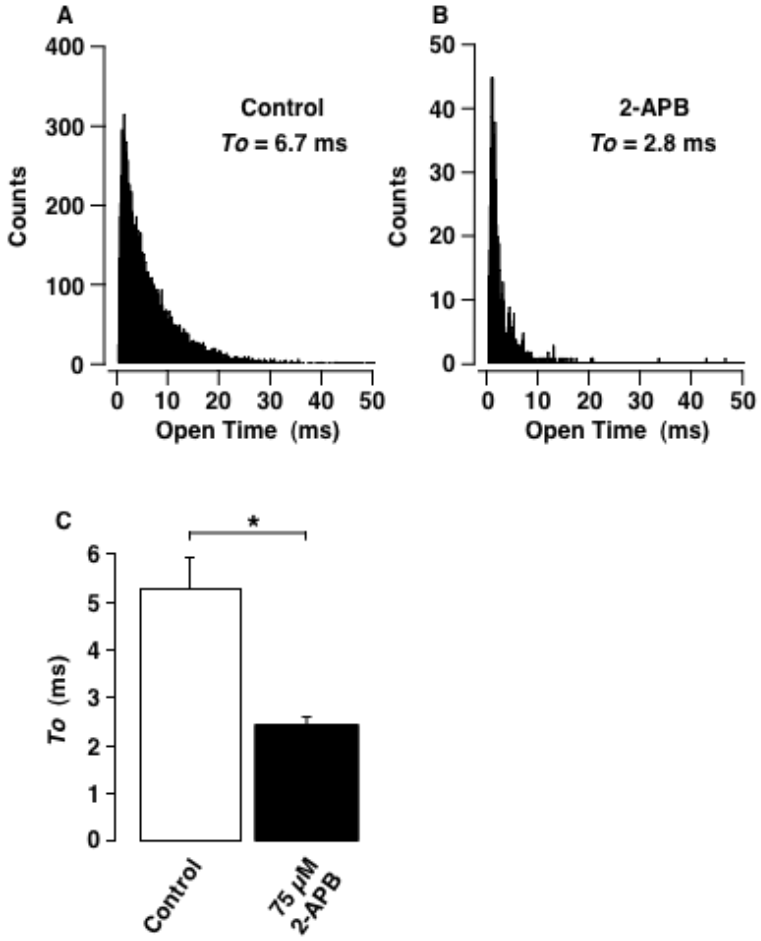
A
400
300
200
100
0
Counts
Control
To = 6.7 ms
0 10 20 30 40 50
Open Time (ms)
B
50
40
30
20
10
0
Counts
2-APB
To = 2.8 ms
0 10 20 30 40 50
Open Time (ms)
C
*
6
5
4
3
2
1
0
To (ms)
Control
75 μM 2-APB

Fig. S1

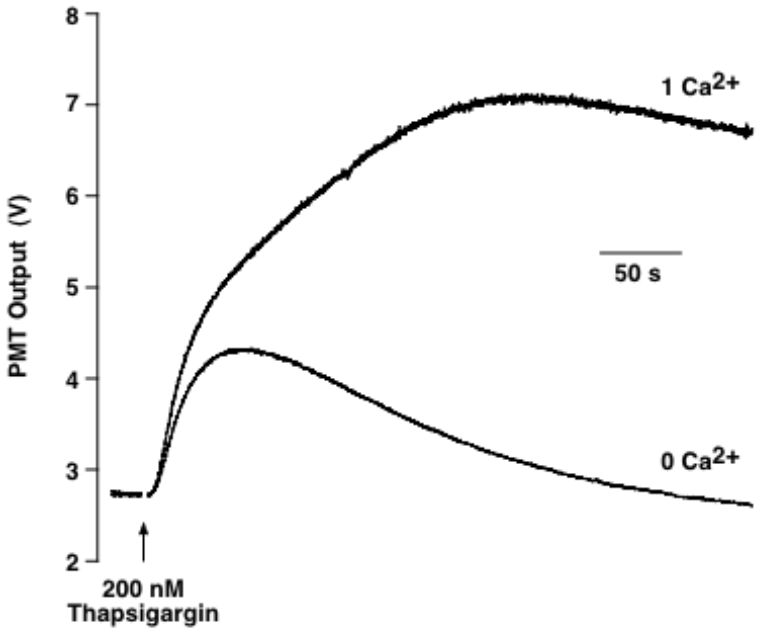

Fig. S2

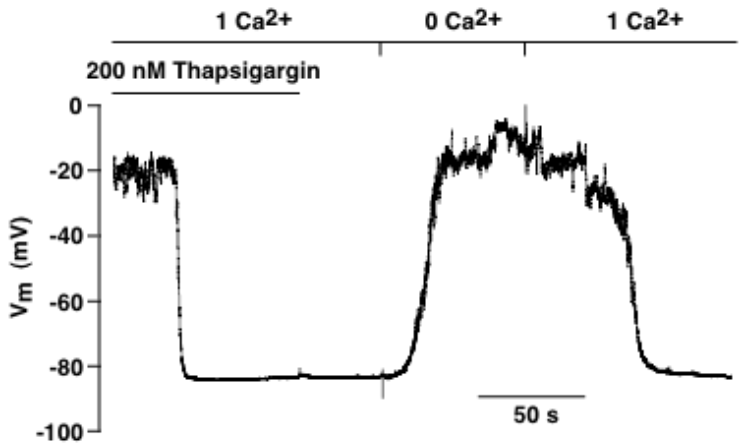

Fig. S3

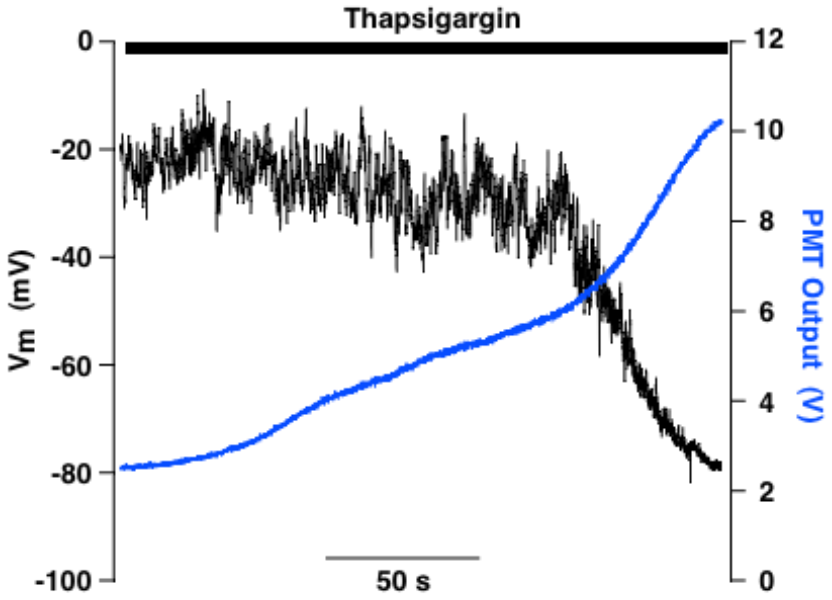
Thapsigargin
0
-20
-40
-60
-80
-100
V_m (mV)
12
10
8
6
4
2
0
PMT Output (V)
50 s

Fig. S4